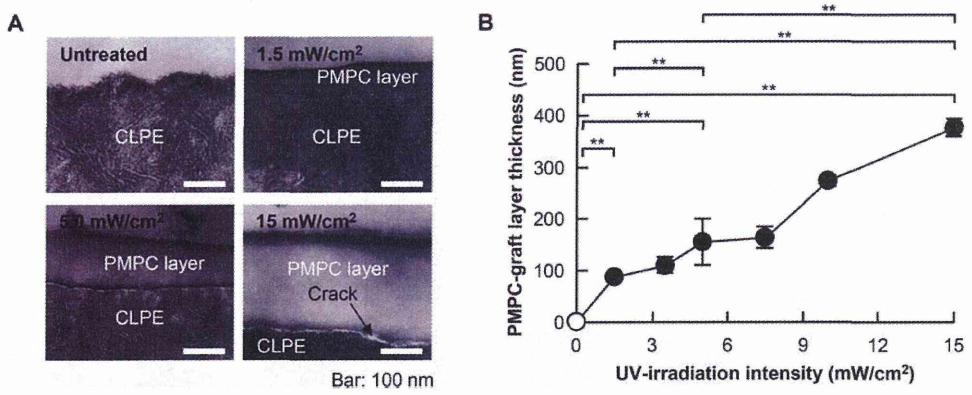

FIGURE 2. (A) Cross-sectional TEM images and (B) PMPC-graft layer thickness of PMPC-grafted CLPE obtained with various UV-irradiation intensities. Open symbol indicates untreated CLPE. Data are expressed as mean ± standard deviation. ** indicates $p < 0.01$.

interface of the PMPC layer and CLPE substrate when a thick polymer layer was formed.

The UV-irradiation intensity affected the hydration and friction kinetics of the PMPC graft layer. The static water contact angle of the untreated CLPE was ~90°, and decreased noticeably with an increase in the UV-irradiation intensity [Fig. 3(A)]. The lowest contact angle observed 30°, which was measured on the samples that was treated at 5.0 mW/cm^2. The angle then increased slightly at higher irradiation intensity. The dynamic coefficients of friction of PMPC-grafted CLPE decreased markedly with an increase in the UV-irradiation intensity, with the surface produced at 3.5–7.5 mW/cm^2 exhibiting an ~85% reduction compared with the untreated CLPE surface [Fig. 3(B)]. However, above 10 mW/cm^2, the values increased slightly. As shown in Figure 4, the dynamic coefficients of friction of the PMPC-grafted CLPE samples obtained using UV-irradiation intensities of 1.5 and 5.0 mW/cm^2 did not differ greatly between loadings, regardless of whether they were gamma-ray sterilized or not. Interestingly, for the nonsterilized PMPC-grafted CLPE obtained with a UV-irradiation intensity of 15 mW/cm^2, the dynamic coefficient of friction in the case of 9.8 N loading was twice as high as that in the case of 0.98 N loading; however, there was no significant difference for the gamma-ray sterilized sample ($p > 0.05$).

Some physical and mechanical properties of PMPC-grafted CLPE as a function of the UV-irradiation intensity are summarized in Figures 5–7. The swelling ratio was almost constant up to an intensity of 10 mW/cm^2, and then decreased slightly above this value [Fig. 5(A)]. The trend in cross-link density also underwent a change at 10 mW/cm^2, gradually increasing up to 0.87 mol % at this point, and then decreasing sharply [Fig. 5(B)]. The ultimate tensile strength and elongation of the untreated CLPE sample differed slightly to the values obtained for the PMPC-grafted CLPE obtained using UV-irradiation intensities of 5.0 and 15 mW/cm^2 [Fig. 6(A,B)]. In contrast, the hardness and impact strength remained almost the same ($p > 0.05$), and appeared to be independent of the UV-irradiation intensity [Fig. 6(C,D)]. The tensile, hardness, and impact resistance properties of all untreated CLPE and PMPC-grafted CLPE samples met the requirements of ASTM F648. The small punch peak strength and work to failure of PMPC-grafted CLPE gradually decreased slightly with UV-irradiation intensity (Fig. 7).

The characteristics of the PMPC-grafted surface affected the durability of the CLPE liners. During the hip simulator

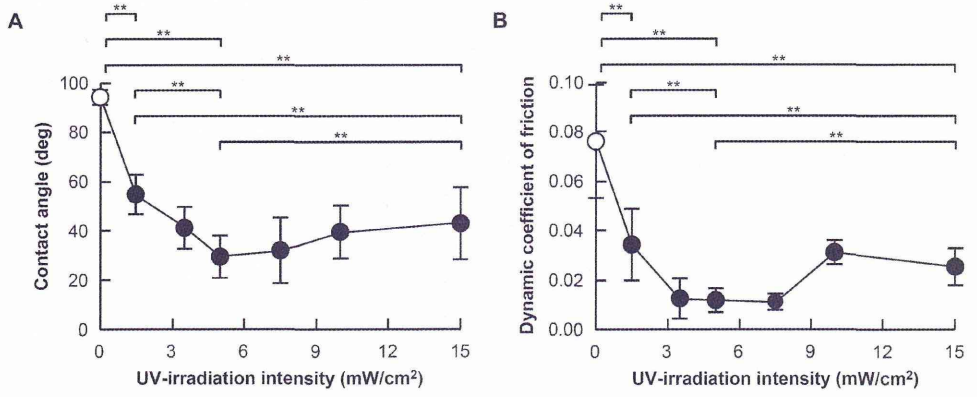

FIGURE 3. (A) Static water contact angle and (B) dynamic coefficient of friction of PMPC-grafted CLPE as a function of the UV-irradiation intensity. Open symbols indicate untreated CLPE. Data are expressed as mean ± standard deviation. ** indicates $p < 0.01$.

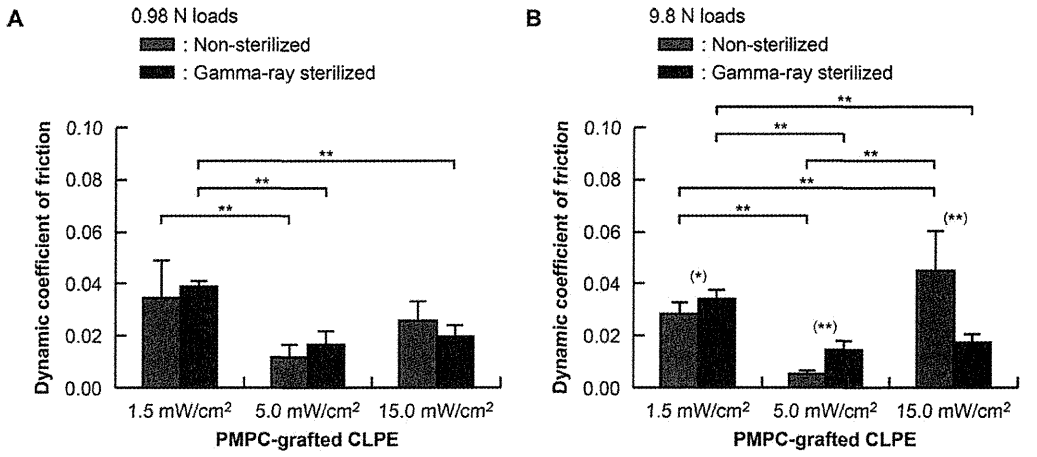

FIGURE 4. Dynamic coefficients of friction of PMPC-grafted CLPE in the ball-on-plate friction test with (A) 0.98 N and (B) 9.8 N loads. Data are expressed as mean ± standard deviation. (*) and (**): *t*-Test, significant differences ($p < 0.05$ and $p < 0.01$, respectively) as a comparison between non-sterilized and gamma-ray sterilized groups, and **: one-factor ANOVA and post-hoc test, significant difference ($p < 0.01$) as comparison between the three groups of the PMPC-grafted CLPE.

wear test, the PMPC-grafted CLPE liner was observed to undergo significantly less gravimetric wear than the untreated CLPE liners [Fig. 8(A)]. Furthermore, there was a slight and gradual increase in weight of the untreated and PMPC-grafted CLPE liners during the testing period, which was partially attributed to greater fluid (e.g., water, proteins, and lipids) absorption by the tested liners than was allowed for by the load-soak controls. As noted earlier, correction using the load-soak control is not perfect because only the tested liners were continuously moved and loaded. Remarkably, extremely small and barely observable wear particles were produced by the PMPC-grafted CLPE liners after 5.0×10^6 cycles ($4.5–5.0 \times 10^6$ cycles) of the hip simulator test [Fig. 8(B)]. The wear particles of the untreated CLPE liners, and the small quantity produced by the PMPC-grafted CLPE, consisted of only sub-micrometer-sized granules. The PMPC grafting did not affect the morphologies of the CLPE wear particles. 3D coordinate measurements of the PMPC-grafted CLPE liners revealed barely detectable volumetric wear, in contrast to the substantial wear detected for the untreated CLPE liners [Fig. 9(A)]. The volumetric wear images in Figure 9(A) are in agreement with the gravimetric wear data shown in Figure 8(A). In the confocal laser scanning microscope images in Figure 9(B), the surface of the untreated CLPE liner against the Co–Cr–Mo alloy femoral head appears smooth. In contrast, the PMPC-grafted CLPE liners exhibit a different morphology; with the machining marks still evident in the bearing surface. There were no differences among the surface morphologies of the three groups of the PMPC-grafted CLPE produced using different UV-irradiation intensities.

DISCUSSION

In this study, we investigated the effects of varying the UV-irradiation intensity on graft polymerization of MPC. The results provide preliminary evidence that the UV-irradiation intensity affected the extent of PMPC grafting and the underlying CLPE substrate. They also demonstrate that the hydrophilic layer increased lubrication to levels that match articular cartilage, and when grafted onto the acetabular liner surface of a THA prosthesis, caused high wear

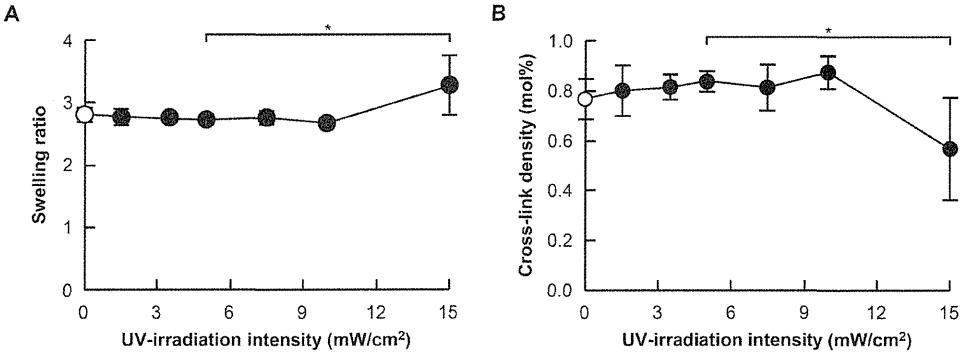

FIGURE 5. (A) Swelling ratio and (B) cross-link density of PMPC-grafted CLPE as a function of UV-irradiation intensity. Open symbols indicate untreated CLPE. Data are expressed as mean ± standard deviation. * indicates $p < 0.05$.

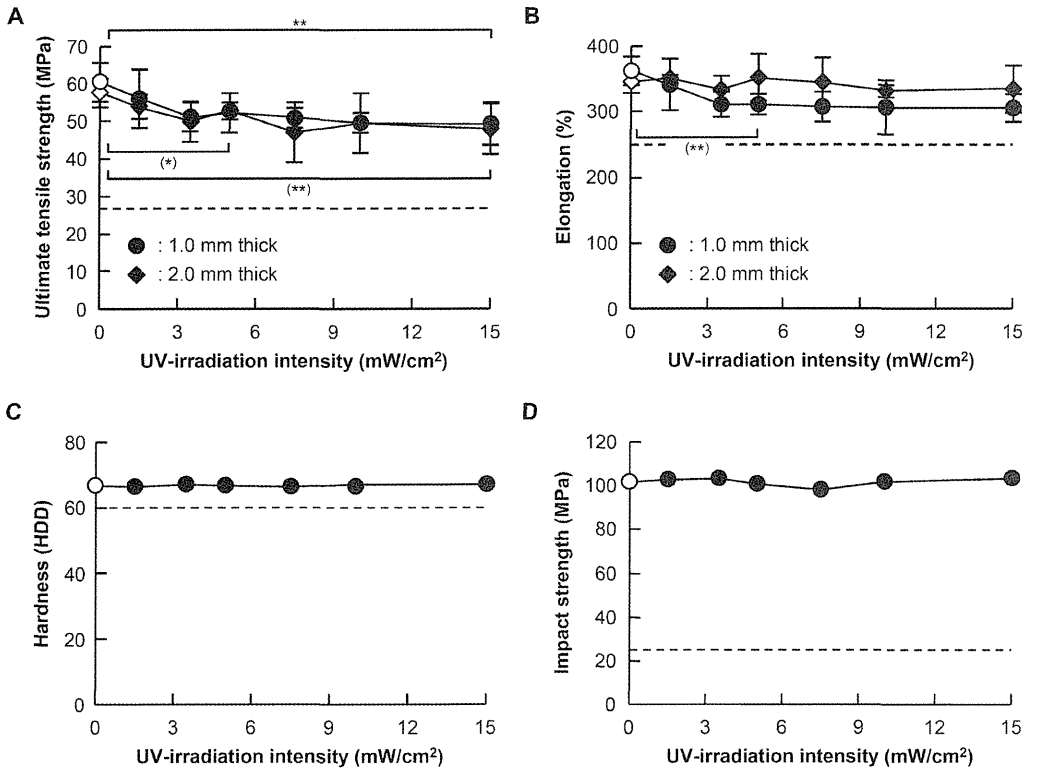

FIGURE 6. Mechanical properties of PMPC-grafted CLPE as a function of UV-irradiation intensity. (A) Ultimate tensile strength; (*) and (**): one-factor ANOVA and post-hoc test, significant difference ($p < 0.05$ and $p < 0.01$, respectively) as compared with the ultimate tensile strength of 1.0 mm thick test specimens, and **: significant difference ($p < 0.01$) of 2.0 mm thick test specimens. (B) Elongation; (**): one-factor ANOVA and post-hoc test, significant difference ($p < 0.01$) as compared to the elongation of 1.0 mm thick test specimens. (C) Hardness and (D) impact strength. Open symbols indicate untreated CLPE. Data are expressed as mean ± standard deviation. Broken lines indicate lower limits of ASTM requirements.

resistance. This suggests the grafting of PMPC may be a promising approach for extending the longevity of THA.

Despite these promising results, our study has a number of limitations. First, *in vitro* findings do not always translate to a clinical success. However, we conducted multicenter clinical trials of PMPC-grafted CLPE liners between 2007 and 2009 in Japan.[22] Based on other related evidence and these clinical trials, the Japanese government (Ministry of

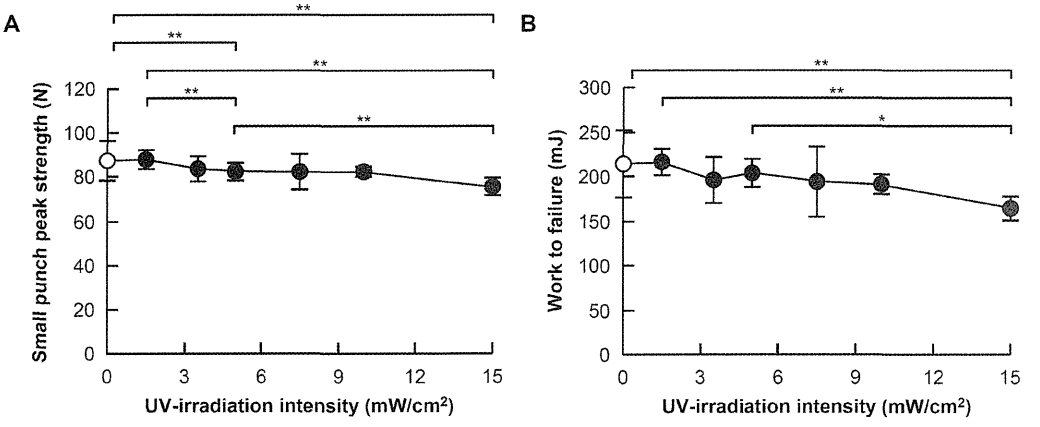

FIGURE 7. Small punch test properties of PMPC-grafted CLPE as a function of UV-irradiation intensity. (A) Small punch peak strength; **: one-factor ANOVA and post-hoc test, significant difference ($p < 0.01$) as compared with the peak strength in four groups of untreated and PMPC-grafted CLPE. (B) Work to failure; * and **: one-factor ANOVA and post-hoc test, significant difference ($p < 0.05$ and $p < 0.01$, respectively) as compared with the work to failure in four groups of untreated and PMPC-grafted CLPE. Open symbols indicate untreated CLPE. Data are expressed as mean ± standard deviation.

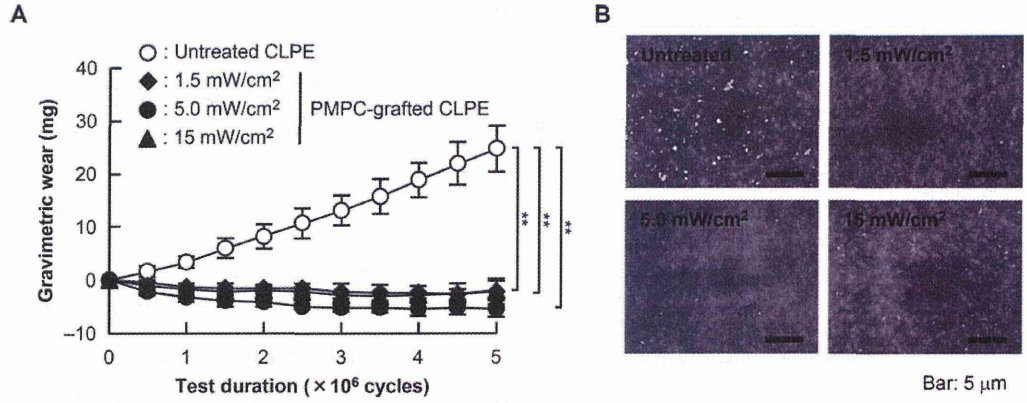

FIGURE 8. A: Time course of the gravimetric wear of the PMPC-grafted CLPE liners obtained using various UV-irradiation intensities. Data are expressed as mean ± standard deviation. **: one-factor ANOVA and post-hoc test, significant difference ($p < 0.01$) as compared with the gravimetric wear after the test in four groups of untreated and PMPC-grafted CLPE. B: SEM images of wear particles from PMPC-grafted CLPE isolated from lubricants of the hip simulator wear test.

Health, Labor, and Welfare, Japan) approved the clinical use of PMPC-grafted CLPE acetabular liners (Aquala® liner; KYOCERA Medical Corp.) in artificial hip joints in April 2011. We observed neither osteolysis nor a need for revision surgery up to 6 years of follow-up. Second, we used a confined period for the hip simulator wear test. Although experiencing 5.0×10^6 cycles in the hip simulator is comparable to 5 years of physical walking, the duration may not be sufficiently long for young active patients. We are now running the hip simulator for longer, and thus far, have confirmed almost no wear on the PMPC-grafted CLPE liners after 1.5×10^7 cycles.[29] Third, we did not entirely capture the range of loading and motion conditions of the *in vivo* environment in terms of the variety of positions, the magnitude of loading, or the daily routine; however, in accordance with ISO 14242-3, we believe that these results can provide a good indication of wear performance. Fourth, the procedure for the isolation of wear particles in this study was not able to capture the contribution of wear particles with a diameter of less than 0.1 μm, as previously reported.[30] Cellular response to particles is thought to be dependent upon factors such as particle number, size, shape, surface area, and material chemistry. If nanometer-scale particles are generated *in vivo*, it will be important to determine their biological activity in relation to that of micrometer-scaled particles. Fifth, the wear performance we report is only valid for this specific combination of Co–Cr–Mo alloy femoral head with a diameter of 26 mm and PMPC-grafted CLPE liner. Although aseptic loosening is one of the most common reasons for late revision surgery, dislocation is the biggest short-term problem.[3] A large femoral head not only allows for an increased head/neck ratio, which is directly related to the

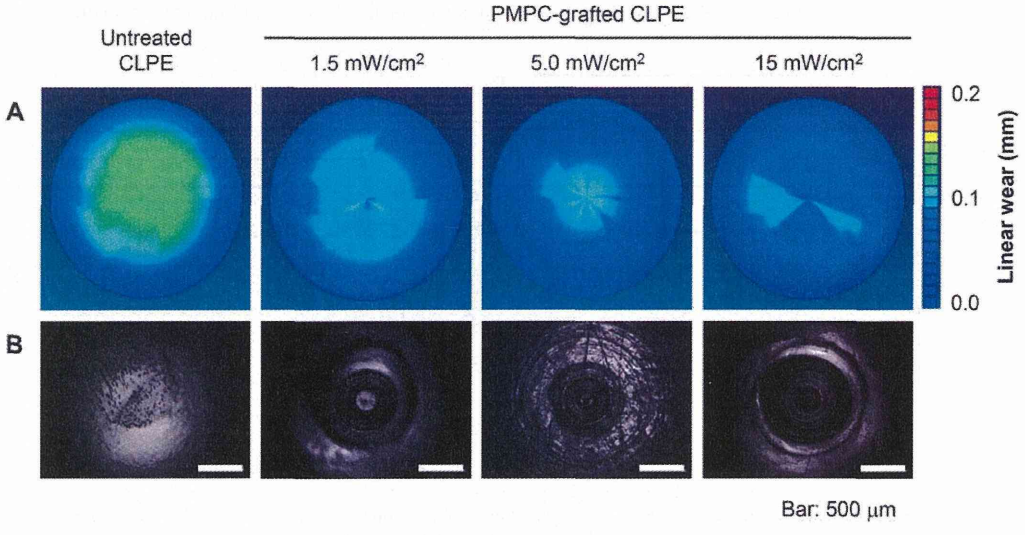

FIGURE 9. (A) 3D coordinate measurement images and (B) confocal laser scanning microscopy images of the PMPC-grafted CLPE liners obtained using various UV-irradiation intensities after 5.0×10^6 cycles. [Color figure can be viewed in the online issue, which is available at wileyonlinelibrary.com.]

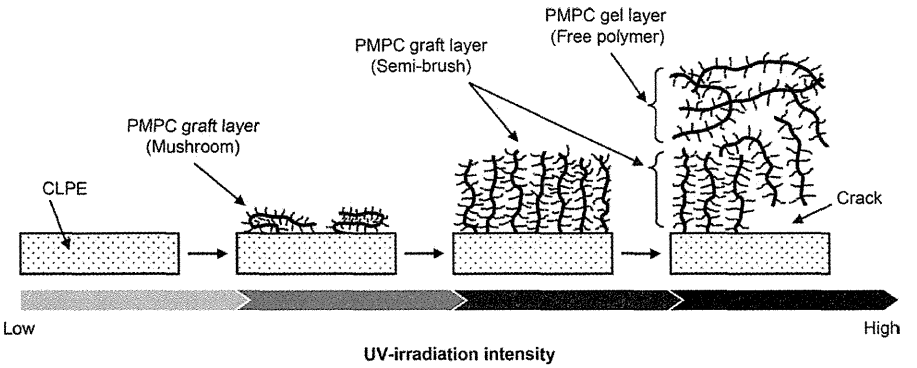

FIGURE 10. Schematic illustration of the PMPC-grafted CLPE surface obtained with various UV-irradiation intensities.

range of motion prior to impingement of the trunnion on the liner, but also increases the jump distance. Hence, larger femoral heads have recently come into more frequent use to improve the stability of the bearing surface. We believe that this drawback is partially offset by the long duration of simulation. We are now running the hip simulator test with larger Co–Cr–Mo alloy and zirconia toughened alumina ceramic femoral heads and thin acetabular liners.

Effects on extent of PMPC grafting

It is important to be able to control the graft layer on CLPE surfaces in order to optimize lubrication and resistance to wear. In Figures 1 and 2, when the MPC concentration and UV-irradiation time were fixed (0.50 mol/L and 90 min), the extent of PMPC grafting on the CLPE surface increased with the UV-irradiation intensity, and then became almost constant at 5.0 atom% over 5.0 mW/cm^2. It is well known that the amount of photoinduced radicals depends on the photo-irradiation intensity[31]; therefore, the extent of grafting appeared to be successfully controlled by varying the quantity of radicals produced during the radical polymerization process. Figure 10 shows a schematic that illustrates how the PMPC grafting is suggested to vary with UV-irradiation intensity during the polymerization.[32] The PMPC graft layer thickness linearly increased with UV-irradiation intensity above 7.5 mW/cm^2, reaching ~380 nm at 15 mW/cm^2. However, as shown in Figure 2(A), the sample produced using 15 mW/cm^2 UV displayed the formation of a crack at the interface between the PMPC layer and CLPE substrate. When the PMPC layer has a semi-brush-like structure (Fig. 10), the layer thickness may correlate with the molecular weight of the grafted PMPC. It is generally known that the reaction rate of radical polymerization is extremely high; therefore, the length (molecular weight) of the graft chains can be assumed to be controlled by the monomer concentration. However, the MPC concentration and UV-irradiation time were fixed in the present study,[27,33] and the graft polymerization reaction with free radicals was photoinduced by UV irradiation using benzophenone as a radical initiator. A certain amount of UV irradiation energy can directly produce free radicals from the methacrylic acid group of the MPC unit in the monomer solution. When the UV-irradiation intensity is high, graft polymerization can occur between the radicals on the CLPE surface and the MPC monomer, in addition to homopolymerization of MPC. The free radicals not only facilitate direct grafting of MPC to CLPE, thereby forming C–C covalent bonds between the PMPC and the CLPE substrate, but also induce homopolymerization of MPC, forming free polymer in solution. Moreover, the diffusion of the monomer might be disrupted in a solution with high homopolymer concentration because of high viscosity. When the monomer and initiator initially attached to the CLPE surface were subjected to UV irradiation, radicals would have freely formed on the CLPE surface in the early stage but not in the late stage of polymerization, probably because the increased polymer radicals and/or free homopolymer chains blocked the diffusion of the radicals to the CLPE surface. Therefore, it is supposed that areas of unmodified CLPE would remain below the PMPC gel (free polymer) layer, which would leave a gap (or crack) at the interface between PMPC and CLPE substrate. In summary, it is assumed that when the UV-irradiation intensity is low (<7.5 mW/cm^2), the rate of MPC graft polymerization is higher than that of MPC homopolymerization. In contrast, when the UV-irradiation intensity is high (>10 mW/cm^2), the rate of homopolymerization might be higher than that of graft polymerization. Moreover, while the rate of MPC graft polymerization increases with the UV-irradiation intensity, the entire polymerization system begins to show gelation, with the formation of PMPC gel layer (on the PMPC graft layer) at UV-irradiation intensities above 10 mW/cm^2, decreasing the grafting efficiency. Therefore, in order to obtain a stable PMPC grafted layer without gelation of PMPC, the UV-irradiation intensity should be carefully controlled.

The water wettabilities of the PMPC-grafted CLPE surfaces were found to be considerably greater than that of the untreated CLPE surfaces [Fig. 3(A)]. This is because of the presence of a nanometer-scale PMPC graft layer resulting from the polymerization of the highly hydrophilic MPC monomer. It can be observed in Figure 3(B) that the dynamic coefficients of friction of the PMPC-grafted CLPE

surfaces were significantly lower than those of the untreated CLPE surface. This was attributed to the significant increase in hydrophilicity evident from the reduction in the static water contact angles of the PMPC-grafted surfaces. The fabrication of the PMPC gel layer clearly influenced the friction response, with the dynamic coefficient of friction for the PMPC-grafted CLPE obtained at 15 mW/cm^2 being less than half of the value for the untreated material at 0.98 N loading. In contrast, at 9.8 N loading, the dynamic coefficient of friction for the 15 mW/cm^2 sample was significantly higher than for those treated at 1.5 and 5.0 mW/cm^2 (Fig. 4). It was previously reported that the dynamic coefficients of friction of MPC polymer coated CLPE prepared by physical adsorption or weak chemical bonding, increased to the level of the untreated CLPE at loads above 1.96 N.[24] It was therefore assumed that these particular surface modification layers became dislodged from the surface at high loading, and were therefore ineffective. In the present study, it is suggested that the PMPC gel layer on the PMPC-grafted CLPE obtained with a UV-irradiation intensity of 15 mW/cm^2 was removed from the bearing surface, resulting in an increase in friction. On the other hand, interestingly, this same sample, but gamma-ray sterilized, expressed high lubricity regardless of loading. In our previous study, we reported that the higher energy radiation used for gamma-ray sterilization induced cross-links not only within the PMPC graft layer, but also between the PMPC graft layer and the CLPE substrate.[34] It was similarly reported that when a high energy beam was irradiated onto a polymer with a grafted layer, strong bonds were formed between the grafted layer and polymer substrate.[35] Moreover, Lewis et al. reported that the force required to remove a coating with cross-linking was greater than that without.[36] Generally, when a high energy gamma-ray beam is irradiated on a polymer, free radicals are formed by the scission of molecular chains.[37] This is followed by the re-termination and cross-linking of the molecules. Hence, it was speculated that in the present study, a higher degree of cross-linking, and perhaps adhesion of PMPC graft and gel layers to the substrate, was induced by the gamma-ray irradiation in comparison to the non-sterilized PMPC-grafted CLPE. This would result in a much stronger and stable PMPC graft layer on the bearing surface.

Effects on CLPE substrate

The tested physical and mechanical properties of CLPE were altered slightly by the PMPC grafting, as shown in Figures 5–7. Most previous studies have assumed that photoinduced polymerization is a surface restricted phenomenon.[26,38] However, in reality, the changes (i.e., cross-linking and chain scission) of the polymer structure under UV radiation can result in changes to the bulk physical and mechanical properties (swelling ratio, cross-link density, and tensile- and small punch-tests properties) of thin test specimens, such as those with a thickness of 0.5–2.0 mm that were used in this study. In the case of the photoinduced cross-linking and scission of the CLPE substrate, one aspect that has been evaluated is the relationship between initiation and the depth of UV penetration. Shyichuk et al. reported that the photoinduced cross-linking and scission of (low-density) PE was observed in the surface region of PE in the range 0–1.5 mm, after UV-irradiation with an intensity of 0.2 mW/cm^2 for over 3 weeks.[26] Hence, it was thought that the observed changes in physical and mechanical properties would be the result of a complex combination of cross-linking and scission effects in a surface restricted region. In particular, it is assumed that when the UV-irradiation intensity is low ($<$7.5 mW/cm^2), the rate of cross-linking is higher than that of chain scission. In contrast, when the UV-irradiation intensity is high ($>$10 mW/cm^2), the rate of scission might be higher than that of cross-linking. However, it should be noted that these phenomena would also be combined with the effects of other polymerization conditions, such as temperature, dissolved oxygen concentration of monomer solution, and photoinitiator concentration. The retention of the bulk properties of the substrates is extremely important in clinical applications because the biomaterials used as implants act not only as surface-functional materials, but also as structural materials *in vivo*. As mentioned above, dislocation is the biggest short-term problem associated with THA.[3] A thin acetabular liner against a large femoral head not only allows for an increased head/neck ratio, which is directly related to the range of motion prior to impingement of the trunnion on the liner, but also increases the jump distance. Hence, the use of implants with such dimensions is becoming more common in order to improve the stability of the bearing surface. Mechanical fracture attributed to scission of the PE molecular backbone in thin acetabular liners of PMPC-grafted CLPE by the possible impingements must therefore be monitored. From the data gathered to date, we have observed neither mechanical fracture nor complications in the clinical use of the PMPC-grafted CLPE liner for a minimum of 4 years and a maximum of 6 years of follow-up.

The production of wear particles in THA is recognized as the main factor behind the initiation of periprosthetic osteolysis and aseptic loosening.[4,5] The inflammatory cellular response to particles is thought to be dependent upon factors such as particle number, size, shape, surface area, and material chemistry. If nanometer-scale particles are produced *in vivo*, it would be important to determine their biological activity relative to that of the micrometer-scale particles. In the wear particle analysis carried out in this study, the collected wear particles from the PMPC-grafted CLPE liners were on the scale of sub-micrometers, regardless of the PMPC grafting and its UV-irradiation intensity. Considering the results of the wear particle analysis, we expect the biological response of the PMPC-grafted CLPE liners *in vivo* to be comparable with those of other conventional untreated CLPE.[39] However, attention must be paid to the abnormal wear particles (sub-micrometer-size and number) in the PMPC-grafted CLPE liner, formed by possible scission reactions of the CLPE substrate. The remarkably fewer wear particles isolated from the lubricants used for the PMPC-grafted CLPE liners compared with those from the lubricants used for the untreated liners may help predict whether the abnormal wear will occur.

High wear resistance of PMPC-grafted CLPE liners

In the hip simulator wear test of the present study, the observed significant improvements in the water wettabilities and frictional properties of the PMPC-grafted CLPE liners resulted in substantial improvements in their wear resistances. The high friction of untreated CLPE surfaces is one of their main disadvantages because it results in greater wear, and possible seizure of bearing couples. The higher frictional properties of untreated CLPE surfaces were found to affect the wear properties, as determined by the hip simulator wear test. In contrast, as noted earlier, the water wettabilities of the PMPC-grafted CLPE surfaces were considerably greater. Fluid film lubrication (or hydration lubrication) of the PMPC-grafted surface was therefore provided by the hydrated layer. The fluid film-forming ability of a 10 nm thick PMPC layer would be equivalent to that of a micrometer-order-thick PMPC layer because the outermost layer is responsible for this property. The hip simulator wear test confirmed that the wear resistance was almost same in each of the three groups of PMPC-grafted CLPE with different PMPC graft layer thicknesses, with the 90 nm thick PMPC graft layer formed at a UV-irradiation intensity of 1.5 mW/cm^2 providing similar wear resistance to the 380 nm thick PMPC graft layer at a UV-irradiation intensity of 15 mW/cm^2. In our previous study, it was found that even a 10 nm thick PMPC graft layer exhibited improved wear resistance.[27] It was therefore speculated that the improved wear resistance was independent of PMPC graft layer thickness. Additionally, the retention of the improved wear resistance of the cross-linked PMPC gel layer combined with PMPC graft layer and/or the substrate (PMPC-grafted CLPE obtained with a UV-irradiation intensity of 15 mW/cm^2) is very interesting. As mentioned above, the cross-links produced by the extra energy of the gamma-rays was effective even for multidirectional high-loading of the hip simulator.

The obtained results confirm that orthopedic bearings using PMPC are able to mimic the natural articular cartilage that protects the joint interface from mechanical wear and facilitates smooth movement of the joints during daily activity.[13] The PMPC structure attracts water in a similar way to the extracellular matrix molecules present in cartilage, providing a lubricating layer on the surface that they are attached to.[15] This study therefore demonstrates the advantages that can be gained from investigating and subsequently mimicking natural structures and systems.

CONCLUSIONS

In this study, we confirmed that the UV-irradiation intensity affected the extent of PMPC grafting, along with cross-linking and scission reactions of the CLPE substrate. The extent of PMPC grafting on the surface of the CLPE gradually increased with increasing UV-irradiation intensity up to 7.5 mW/cm^2, and then remained constant above this value. It was found that in order to obtain a stable PMPC grafted layer without gelation of PMPC, the UV-irradiation intensity needed to be carefully controlled. When the CLPE surface under the grafted polymer was exposed to UV-irradiation, some of the physical and mechanical properties of the CLPE were altered slightly due to cross-linking and scission effects in the surface region. The hydrophilic PMPC layer grafted onto the CLPE surface significantly increased lubrication to levels that match articular cartilage. By mimicking the properties of the extracellular matrix of cartilage, the high wear resistance of the native tissue could be replicated by the use of an artificial polymer.

ACKNOWLEDGMENTS

The authors thank Mr. Takeshi Nizuka, Mr. Kenichi Saiga, and Mr. Kenichi Watanabe of KYOCERA Medical Corp. for their technical assistance. They further express our gratitude to Prof. Dr. Kozo Nakamura of the National Rehabilitation Center for Persons with Disabilities, Prof. Dr. Sakae Tanaka and Dr. Hiroshi Kawaguchi of the University of Tokyo for their valuable discussions and suggestions.

REFERENCES

1. Kurtz S, Mowat F, Ong K, Chan N, Lau E, Halpern M. Prevalence of primary and revision total hip and knee arthroplasty in the United States from 1990 through 2002. J Bone Joint Surg Am 2005;87:1487–1497.
2. Harris WH. The problem is osteolysis. Clin Orthop Relat Res 1995; 311:46–53.
3. Bozic KJ, Kurtz SM, Lau E, Ong K, Vail TP, Berry DJ. The epidemiology of revision total hip arthroplasty in the United States. J Bone Joint Surg Am 2009;91:128–133.
4. Sochart DH. Relationship of acetabular wear to osteolysis and loosening in total hip arthroplasty. Clin Orthop Relat Res 1999; 363:135–150.
5. Jacobs JJ, Roebuck KA, Archibeck M, Hallab NJ, Glant TT. Osteolysis: basic science. Clin Orthop Relat Res 2001;393:71–77.
6. McMinn DJ, Daniel J, Pynsent PB, Pradhan C. Mini-incision resurfacing arthroplasty of hip through the posterior approach. Clin Orthop Relat Res 2005;441:91–98.
7. Muratoglu OK, Bragdon CR, O'Connor DO, Jasty M, Harris WH. A novel method of cross-linking ultra-high-molecular-weight polyethylene to improve wear, reduce oxidation, and retain mechanical properties. Recipient of the 1999 HAP Paul Award. J Arthroplasty 2001;16:149–160.
8. Kyomoto M, Iwasaki Y, Moro T, Konno T, Miyaji F, Kawaguchi H, Takatori Y, Nakamura K, Ishihara K. High lubricious surface of cobalt-chromium-molybdenum alloy prepared by grafting poly(2-methacryloyloxyethyl phosphorylcholine). Biomaterials 2007;28: 3121–3130.
9. Kyomoto M, Moro T, Saiga K, Miyaji F, Kawaguchi H, Takatori Y, Nakamura K, Ishihara K. Lubricity and stability of poly(2-methacryloyloxyethyl phosphorylcholine) polymer layer on Co-Cr-Mo surface for hemi-arthroplasty to prevent degeneration of articular cartilage. Biomaterials 2010;31:658–668.
10. Kyomoto M, Moro T, Takatori Y, Kawaguchi H, Nakamura K, Ishihara K. Self-initiated surface grafting with poly(2-methacryloyloxyethyl phosphorylcholine) on poly(ether-ether-ketone). Biomaterials 2010;31:1017–1024.
11. Kyomoto M, Moro T, Yamane S, Hashimoto M, Takatori Y, Ishihara K. Poly(ether-ether-ketone) orthopedic bearing surface modified by self-initiated surface grafting of poly(2-methacryloyloxyethyl phosphorylcholine). Biomaterials 2013;34:7829–7839.
12. Levine BR, Hsu AR, Skipor AK, Hallab NJ, Paprosky WG, Galante JO, Jacobs JJ. Ten-year outcome of serum metal ion levels after primary total hip arthroplasty: A concise follow-up of a previous report*. J Bone Joint Surg Am 2013;95:512–518.
13. Kirk TB, Wilson AS, Stachowiak GW. The morphology and composition of the superficial zone of mammalian articular cartilage. J Orthop Rheumatol 1993;6:21–28.

14. Kyomoto M, Moro T, Saiga K, Hashimoto M, Ito H, Kawaguchi H, Takatori Y, Ishihara K. Biomimetic hydration lubrication with various polyelectrolyte layers on cross-linked polyethylene orthopedic bearing materials. Biomaterials 2012;33:4451–4459.
15. Goldberg R, Schroeder A, Silbert G, Turjeman K, Barenholz Y, Klein J. Boundary lubricants with exceptionally low friction coefficients based on 2D close-packed phosphatidylcholine liposomes. Adv Mater 2011;23:3517–3521.
16. Ishihara K, Ueda T, Nakabayashi N. Preparation of phospholipid polymers and their properties as polymer hydrogel membranes. Polym J 1990;22:355–360.
17. Ishihara K, Aragaki R, Ueda T, Watenabe A, Nakabayashi N. Reduced thrombogenicity of polymers having phospholipid polar groups. J Biomed Mater Res 1990;24:1069–1077.
18. Ishihara K, Ziats NP, Tierney BP, Nakabayashi N, Anderson JM. Protein adsorption from human plasma is reduced on phospholipid polymers. J Biomed Mater Res 1991;25:1397–1407.
19. Kuiper KK, Nordrehaug JE. Early mobilization after protamine reversal of heparin following implantation of phosphorylcholine-coated stents in totally occluded coronary arteries. Am J Cardiol 2000;85:698–702.
20. Selan L, Palma S, Scoarughi GL, Papa R, Veeh R, Di Clemente D, Artini M. Phosphorylcholine impairs susceptibility to biofilm formation of hydrogel contact lenses. Am J Ophthalmol 2009;147: 134–139.
21. Snyder TA, Tsukui H, Kihara S, Akimoto T, Litwak KN, Kameneva MV, Yamazaki K, Wagner WR. Preclinical biocompatibility assessment of the EVAHEART ventricular assist device: Coating comparison and platelet activation. J Biomed Mater Res A 2007;81:85–92.
22. Takatori Y, Moro T, Kamogawa M, Oda H, Morimoto S, Umeyama T, Minami M, Sugimoto H, Nakamura S, Karita T, Kim J, Koyama Y, Ito H, Kawaguchi H, Nakamura K. Poly(2-methacryloyloxyethyl phosphorylcholine)-grafted highly cross-linked polyethylene liner in primary total hip replacement: One-year results of a prospective cohort study. J Artif Organs 2013;16:170–175.
23. Ishihara K, Iwasaki Y, Ebihara S, Shindo Y, Nakabayashi N. Photoinduced graft polymerization of 2-methacryloyloxyethyl phosphorylcholine on polyethylene membrane surface for obtaining blood cell adhesion resistance. Colloids Surf B Biointerfaces 2000;18(3-4):325–335.
24. Kyomoto M, Moro T, Miyaji F, Hashimoto M, Kawaguchi H, Takatori Y, Nakamura K, Ishihara K. Effects of mobility/immobility of surface modification by 2-methacryloyloxyethyl phosphorylcholine polymer on the durability of polyethylene for artificial joints. J Biomed Mater Res A 2009;90:362–371.
25. Fallani F, Ruggeri G, Bronco S, Bertoldo M. Modification of surface and mechanical properties of polyethylene by photo-initiated reactions. Polym Degrad Stab 2003;82:257–261.
26. Shyichuk AV, White JR, Craig IH, Syrotynska ID. Comparison of UV-degradation depth-profiles in polyethylene, polypropylene and an ethylene–propylene copolymer. Polym Degrad Stab 2005; 88:415–419.
27. Kyomoto M, Moro T, Miyaji F, Hashimoto M, Kawaguchi H, Takatori Y, Nakamura K, Ishihara K. Effect of 2-methacryloyloxyethyl phosphorylcholine concentration on photo-induced graft polymerization of polyethylene in reducing the wear of orthopaedic bearing surface. J Biomed Mater Res A 2008;86:439–447.
28. Kyomoto M, Moro T, Konno T, Takadama H, Kawaguchi H, Takatori Y, Nakamura K, Yamawaki N, Ishihara K. Effects of photo-induced graft polymerization of 2-methacryloyloxyethyl phosphorylcholine on physical properties of cross-linked polyethylene in artificial hip joints. J Mater Sci Mater Med 2007;18:1809–1815.
29. Moro T, Kyomoto M, Ishihara K, Saiga K, Hashimoto M, Tanaka S, Ito H, Tanaka T, Oshima H, Kawaguchi H, Takatori Y. Grafting of poly(2-methacryloyloxyethyl phosphorylcholine) on polyethylene liner in artificial hip joints reduces production of wear particles. J Mech Behav Biomed Mater. Forthcoming.
30. Tipper JL, Galvin AL, Williams S, McEwen HM, Stone MH, Ingham E, Fisher J. Isolation and characterization of UHMWPE wear particles down to ten nanometers in size from in vitro hip and knee joint simulators. J Biomed Mater Res A 2006;78: 473–480.
31. Gruber HF. Photoinitiators for free radical polymerization. Prog Polym Sci 1992;17:953–1044.
32. Kyomoto M, Moro T, Takatori Y, Kawaguchi H, Ishihara K. Cartilage-mimicking, high-density brush structure improves wear resistance of crosslinked polyethylene: A pilot study. Clin Orthop Relat Res 2011;469:2327–2336.
33. Kyomoto M, Moro T, Konno T, Takadama H, Yamawaki N, Kawaguchi H, Takatori Y, Nakamura K, Ishihara K. Enhanced wear resistance of modified cross-linked polyethylene by grafting with poly(2-methacryloyloxyethyl phosphorylcholine). J Biomed Mater Res A 2007;82:10–17.
34. Kyomoto M, Moro T, Miyaji F, Konno T, Hashimoto M, Kawaguchi H, Takatori Y, Nakamura K, Ishihara K. Enhanced wear resistance of orthopaedic bearing due to the cross-linking of poly(MPC) graft chains induced by gamma-ray irradiation. J Biomed Mater Res B Appl Biomater 2008;84:320–327.
35. Salleh NG, Glasel HJ, Mehnert R. Development of hard materials by radiation curing technology. Radiat Phys Chem 2002;63(3–6): 475–479.
36. Lewis AL, Cumming ZL, Goreish HH, Kirkwood LC, Tolhurst LA, Stratford PW. Crosslinkable coatings from phosphorylcholine-based polymers. Biomaterials 2001;22:99–111.
37. Costa L, Luda MP, Trossarelli L, Brach del Prever EM, Crova M, Gallinaro P. Oxidation in orthopaedic UHMWPE sterilized by gamma-ray radiation and ethylene oxide. Biomaterials 1998; 19(7–9):659–668.
38. Giesse R, De Paoli MA. Surface and bulk oxidation of low-density polyethylene under UV-irradiation. Polym Degrad Stab 1988;21: 181–187.
39. Moro T, Takatori Y, Ishihara K, Konno T, Takigawa Y, Matsushita T, Chung UI, Nakamura K, Kawaguchi H. Surface grafting of artificial joints with a biocompatible polymer for preventing periprosthetic osteolysis. Nat Mater 2004;3:829–837.

Special Issue Article

Institution of MECHANICAL ENGINEERS

Journal of ENGINEERING TRIBOLOGY

Proc IMechE Part J:
J Engineering Tribology
0(0) 1–13

DOI: 10.1177/1350650114530273
pij.sagepub.com

SAGE

Superior lubricity in articular cartilage and artificial hydrogel cartilage

Teruo Murakami[1], Seido Yarimitsu[1], Kazuhiro Nakashima[2], Tetsuo Yamaguchi[2], Yoshinori Sawae[2], Nobuo Sakai[3] and Atsushi Suzuki[4]

Abstract

In healthy natural synovial joints, the extremely low friction and minimum wear are maintained by their superior load-carrying capacity and lubricating ability. This superior lubricating performance appears to be actualized not by single lubrication mode but by synergistic combination of multimode mechanisms such as fluid film, biphasic, hydration, gel film and/or boundary lubrication. On the contrary, in most artificial joints composed of ultra-high molecular weight polyethylene against metal or ceramic-mating material, boundary and/or mixed lubrication modes prevail and thus local direct contact brings down high friction and high-wear problems. To extend the durability of artificial joint, the reduction in friction and wear by improvement in lubrication mechanism is required as an effective design solution. In this paper, at the start, the mechanism of superior lubricity for articular cartilage is examined from the viewpoints of biphasic and boundary lubrication mechanism. Subsequently, the proposal of biomimetic artificial hydrogel cartilage is put forward to improve the lubricating modes in artificial joints. The tribological behaviours in two kinds of poly(vinyl alcohol) hydrogels are compared with that of natural cartilage. The importance in lubrication mechanism in artificial hydrogel cartilage is discussed.

Keywords

Biotribology, articular cartilage, artificial cartilage, hydrogel, biphasic lubrication, boundary lubrication

Date received: 30 November 2013; accepted: 11 March 2014

Introduction

In human musculoskeletal system with the multimodal smooth movements, the extremely low friction and minimum wear in natural synovial joints appear to be maintained not by a single lubrication mode but by the synergistic combination of various modes from fluid-film lubrication to boundary lubrication.[1–3] As important lubrication modes correspond to the severity in daily activities, micro-elastohydrodynamic lubrication,[4] biphasic,[5,6] hydration,[7,8] boundary,[9–11] gel-film lubrication[12] and others are expected to become adaptively effective. Therefore, this lubrication mechanism is called adaptive multimode lubrication.[3,13,14] In natural synovial joints, the synergistic mechanism of articular cartilage and synovial fluid brings about effective superior lubrication. The authors focus in particular the importance of adsorbed film formation on cartilage surface and biphasic lubrication. To clarify the influence of boundary lubrication by adsorbed film, they selected severer reciprocating condition with gradual increase in friction for articular cartilage under continuous loading. In reciprocating test of ellipsoidal articular cartilage against flat glass plate including restarting test after interruption and unloading, Murakami et al.[15] showed the effectiveness of coexistence of γ-globulin and hyaluronic acid (HA) in lowering friction through adsorbed film formation compared with HA solution. In contrast, the coexistence of albumin and HA increased to higher friction level than HA solution due to the interaction of albumin and HA. Even under rubbing lubricated with HA solution containing γ-globulin, however, the friction after each 36-m sliding attained to still high level of 0.1 as

[1]Research Center for Advanced Biomechanics, Kyushu University, Fukuoka, Japan
[2]Department of Mechanical Engineering, Kyushu University, Fukuoka, Japan
[3]Department of Applied Science for Integrated System Engineering, Graduate School of Engineering, Kyushu Institute of Technology, Kitakyushu, Japan
[4]Department of Materials Science and Research Institute of Environment and Information Sciences, Yokohama National University, Yokohama, Japan

Corresponding author:
Teruo Murakami, Research Center for Advanced Biomechanics, Kyushu University, 744 Motooka, Nishi-ku, Fukuoka 819-0395, Japan.
Email: tmura@mech.kyushu-u.ac.jp

coefficient of friction. In a subsequent study,[16] it was shown that the HA solution containing phospholipid, albumin and γ-globulin as appropriate concentrations similar to synovial fluid could maintain superior low-friction level of 0.01 as coefficient of friction and minimum wear in reciprocating test of articular cartilage. This result clarified the importance of adsorbed film formation with superior lubricity in thin-film lubrication.

On the biphasic lubrication mechanism for reciprocating cylindrical indenter on flat articular cartilage, Sakai et al.[17] estimated time-dependent changes in interstitial fluid pressure and von Mises stress in cartilage based on the biphasic finite element (FE) analysis, in which model properties for depth-dependent compressive modulus,[18] addition of spring element[19] corresponding to collagen reinforcement in tensile strain and strain-dependent permeability[19] were included. The material properties in FE model were estimated in cylindrical indentation test under wide condition including physiologically high speed. They pointed out that higher proportion of fluid load support can be sustained by biphasic lubrication mechanism in cartilage under migrating contact condition even at low-sliding speed such as 4 mm/s where hydrodynamic effect lapses. Furthermore, the improvement of fluid load support by fibre reinforcement in sliding condition was indicated. In this paper, particularly the effectiveness of biphasic lubrication in natural synovial joints is described in relation to boundary lubrication.

On the contrary, in artificial joints composed of ultra-high molecular weight polyethylene (UHMWPE) and metal or ceramic material, the mixed or boundary lubrication mode functions predominantly in daily activities, some direct contacts between rubbing surfaces occur and thus increase friction and induce considerable wear. Although the durability of over 15 years becomes established for most cases in clinical application of joint replacements for hip and knee joints, the joint loosening caused by wear debris-induced osteolysis[20,21] has required considerable patients to undergo revision surgery. Additionally, it is noteworthy that high friction on rubbing surfaces accelerates the surface failure and the joint loosening. Therefore, the prevention of wear and the reduction of friction are strongly required to improve the longevity of joint prostheses in clinical application. Although several methods such as crosslinking,[22] addition of vitamin E[23] and surface treatment by phospholipid polymer[24] to UHMWPE have considerably reduced wear and extended the life of joint prostheses, there are still unsolved problems on wear. For hard-on-hard hip prostheses such as metal-on-metal and ceramic-on-ceramic, the upgrading in material properties with high-wear resistance, better surface finish and good design improved clinical performances accompanied with beneficial fluid-film lubrication, but in certain cases, severe problems occurred as stripe wear under edge loading and/or malposition, release of metallic ions, pseudotumor, breakage of ceramic components, squeaking and so on. Besides, the lowering of friction is not always satisfactory. Therefore, alternate method to establish minimum wear and low friction in artificial joints is required.

In order to fundamentally improve the lubrication modes in artificial joints, the applications of various compliant artificial cartilage materials as cartilage replacement have been developed. The application of appropriate compliant artificial cartilage materials with properties similar to articular cartilage is expected to duplicate the superior load-carrying capacity and lubricating ability of natural synovial joints. The lowering of elastic modulus as 1–30 MPa or so as rubbing compliant materials from 800 MPa or so of UHMWPE not only can reduce the contact stress level but also can enhance the fluid-film formation due to the significant elastic deformation effect. Dowson[25] indicated the importance of compliant material properties with proposal as cushion bearing or cushion form bearing. Unsworth et al.[26] showed clear difference in frictional behaviours between UHMWPE and polyurethane acetabular surfaces in hip-joint replacements in experimental simulator tests. For hip prostheses lined with polyurethane of appropriate compliance and thickness, the fluid-film lubrication could be achieved even with low-viscosity lubricants from 0.002 to 0.071 Pa s. In the authors' previous study[27] on walking simulator tests of knee prostheses to evaluate the fluid-film formation between metallic femoral and conductive tibial components with electric resistance method, the significant fluid-film formation except slight drops at flexion stroke ends during stance phase was confirmed for silicone rubber tibial layer with elastic modulus of 9.1 MPa lubricated with silicone oil of 0.1 Pa s. In contrast, intimate contact occurred during full walking phase for anatomical knee prosthesis with UHMWPE tibial component lubricated even with high-viscosity silicone oils of 10 Pa s. This fact indicates the superiority in fluid-film formation due to soft-EHL effect with compliant silicone rubber. With decreasing of lubricant viscosity to 0.01 Pa s, however, local intimate direct contact occurred in knee prosthesis with silicone rubber tibial component. It is generally pointed out that porous hydrogels as water-swollen crosslinked hydrophilic polymers give lower friction than non-porous silicone rubber and polyurethane at start-up or after breakdown of the fluid film. The articular cartilage in natural synovial joints is considered as one of natural hydrogel containing high-water content. The application of hydrogel as cartilage replacement is expected to mimic the lubricious articular cartilage.

In 1988, Sasada[28] reported that the hip prosthesis with poly(vinyl alcohol) (PVA) hydrogel layer prepared by repeated freeze-thawing method with

85–90 wt% water content showed quite similar low-frictional behaviour to natural synovial joint, but did not attain the sufficient durability for clinical application. In contrast, Oka et al.[29] had better wear resistance in uni-directional pin-on-disc (alumina) test by applying the PVA hydrogel prepared through other synthetic process with lower water content, but wear increased in reciprocating test including thin-film conditions at stroke ends. In a subsequent study,[30] the treatment such as cross-linking by γ-radiation or high-pressure injection moulding, the mechanical properties were improved, but the combination of PVA hydrogel with low-water content against itself showed high friction. Therefore, this hydrogel was applicable as a mating material in hemiarthroplasty and artificial meniscus because of its low-friction property against articular cartilage.

Murakami et al.[31] showed in simulator test that the knee prosthesis model with PVA hydrogel layer prepared by repeated freeze-thawing method with high-water content of 79 wt% and Young's modulus of 1.1 MPa exhibited superior lower friction in walking condition lubricated with hyaluronate (HA) solution containing serum protein than for the model with polyurethane layer with elastic modulus of 40 MPa. The minimum fluid-film thickness considering elastic deformation effect for PVA hydrogel is estimated as 0.75 μm during walking, while that for the polyurethane layer exhibits thinner film than 0.2 μm. Maximum coefficient of friction for PVA hydrogel during stance phase was less than about 0.01, but that for polyurethane became higher than 0.2. The superiority of PVA hydrogel should be considered from the viewpoints of surface and biphasic properties in addition to difference in fluid-film thickness.

In reciprocating tests under thin-film condition,[32,33] even PVA hydrogel of high-water content showed significant wear in HA solutions. In reciprocating tests for PVA hydrogel against itself,[33] the addition of single protein in HA solutions increased wear of PVA with increasing concentration. However, at appropriate concentration ratio and concentration of albumin and γ-globulin in lubricants, the wear was remarkably minimized, where the layered adsorbed film was formed as shown by fluorescent images of adsorbed films after testing.[33] At high-wear condition, heterogeneous adsorbed films were formed. Subsequently, the time-dependent adsorbed film formation during reciprocation was confirmed by in situ visualization.[34] In the observation by using total internal reflection fluorescence microscopy, it was shown that the bottom layer composed of γ-globulin plays an important role in stability of mixed protein adsorbed films under rubbing condition. Furthermore, the coexistence of γ-globulin with HA enhanced the adsorption of HA on PVA and glass surfaces. The formation of adsorbed films with optimum structure is an important factor to establish longer durability of hydrogel. The improvement in strength of hydrogel is still required.

To enhance the strength of hydrogels, the chemical crosslinking treatments have been applied. Various semi-interpenetrating network (SIPN) hydrogel materials were synthesized by polymerizing a mixture of lightly crosslinked, vinyl monomers around a reinforcing polymer. Corkhill et al.[35] developed SIPN hydrogels of N-vinylpyrrolidone (NVP) and methyl methacrylate (MMA) as candidate materials with similar strength to natural articular cartilage. The friction and wear properties were evaluated in simulator and reciprocating tests[32] for flat specimens of different reinforcing polymers of polyurethane (pellethane) and cellulose acetate (CA), i.e. NVP–MMA–pellethane (Young's modulus: $E = 21$ MPa, water content: 40 wt%) and NVP–MMA–CA ($E = 23$ MPa, water content: 50 wt%). SIPN hydrogel showed higher friction and higher wear than those for freeze-thawing PVA hydrogel with high-water content. These results suggest the existence of optimum conditions of elastic modulus and water content for low friction and minimum wear. Furthermore, the importance of surface lubricity should be noticed.

Double network (DN) hydrogel composed of two kinds of hydrophilic polymers is another candidate material with higher strength but high-water content. DN hydrogel consists of the combination of stiff and brittle first network and soft and ductile second network. The hydrogel materials have elastic modulus of 0.4 to 0.9 MPa and exhibit the compressive fracture strength as high as a few to several tens of MPa, in spite of high-water content (90%). The application for hemiarthroplasty is developed as possible application.[36]

Although various kinds of hydrogel as cartilage replacement have been developed, clinical application has not yet been completed. To extend the longevity of joint prostheses with artificial hydrogel cartilage, the improvement of tribological properties of artificial cartilage materials is required under various operating conditions in daily activities.

In this study, the mechanisms with superior lubricity in both natural and artificial cartilage materials containing high-water content are explored particularly from the viewpoints of biphasic and boundary lubrication. The tribological behaviours in two kinds of PVA hydrogel materials prepared by repeated freeze–thawing method and cast-drying method were compared with natural cartilage.

Materials and methods

Materials

As stationary ellipsoidal specimens against a reciprocating flat glass plate (a slide glass) in reciprocating test, the natural articular cartilage and two kinds of artificial hydrogel cartilage specimens were prepared as follows:

Articular cartilage. The intact ellipsoidal articular cartilage specimens with subchondral layer were prepared

from the femoral condyle of porcine knee joints (6 to 7 months old) (Figure 1(a)). Before testing, cartilage specimen surfaces were washed with a saline solution in order to remove any eventual residue of synovial joint fluid.

Artificial cartilage. In this study, two kinds of PVA hydrogel materials prepared by repeated freeze-thawing method and cast-drying method were used as described below.

1. PVA hydrogel by repeated freeze-thawing method (Figure 1(b)).[33,34,37]
   PVA (Kishida Chemical Co. Ltd., Japan) used in this method has the polymerization degree of 2000 and an average degree of saponification of 98.4–99.8 mol%. PVA powder at 20 wt% was dissolved in pure water and heated at 120°C for 30 min in autoclave and cast in a mould in air to control the specimen thickness and then gelled by repeated freeze-thawing (for 10 h at −20°C to for 20 h at 4°C) method. Number of freezing-thawing cycles was five times as optimum condition to establish maximum tensile strength and stiffness.[37] The elastic modulus of PVA hydrogel is 1.2 MPa, and equivalent water content is 79%.
2. PVA hydrogel by cast-drying method (Figure 1(c)).[38,39]
   PVA (Kuraray Co. Ltd., Japan) used in this method has the polymerization degree of 1700 and average degree of saponification of 98–99 mol%. An aqueous PVA solution was obtained by dissolving 15.0 wt% of the PVA powder into deionized and distilled water at 90°C for more than 2 h. The PVA solution was poured into a plastic dish of polyethylene and left in air at room temperature (ca. 25°C). The solution became very viscous within several days and solidified within a week or more. The sample was usually prepared by the process of repeated water exchange with drying.

Reciprocating tests of articular cartilage and artificial cartilage

The reciprocating tests of stationary articular cartilage and artificial hydrogel cartilage specimens were conducted against reciprocating flat glass plate.

1. Articular cartilage specimens composed of ellipsoidal condyle with subchondral bone.
2. Artificial cartilage specimens composed of a 2-mm thick soft layer of PVA hydrogel adhered on acrylic ellipsoid (40 mm × 25 mm, in diameter).

In the reciprocating apparatus,[15,16] the sliding speed and stroke length were 20 mm/s and 35 mm, respectively. Applied load was 2.94 N or 9.8 N. Sliding distance for continuous test was 36 m or 140 m. In repeated test in interval of 36 m, the reciprocating sliding was started immediately after loading and interrupted after 514 cycles at sliding distance of 36 m, and then the unloading state was maintained for 5 min. Subsequently, the reciprocating test was restarted immediately after reloading and continued for a further sliding distance of 36 m. The restarting processes were repeated three times. The lubricants are saline or saline solutions containing L-α-dipalmitoyl phosphatidyl-choline (DPPC) as liposomes, serum protein (albumin and γ-globulin) and/or HA (molecular weight: 9.2×10^5).[16]

Biphasic FE analyses for articular cartilage and artificial cartilage

By applying the method of biphasic FE analysis for articular cartilage in reciprocating rubbing by Sakai et al.,[17] two-dimensional FE analysis for cylindrical articular cartilage or PVA hydrogel cartilage was conducted under continuous loading by impermeable rigid plate in reciprocating motion as shown in Figure 2.[14] The thickness of soft layer is 1.5 mm and

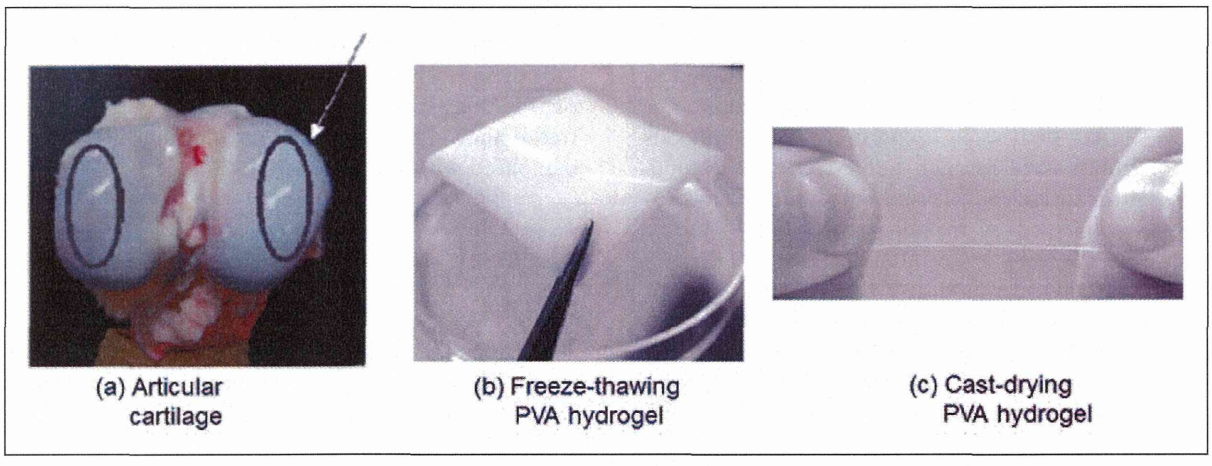

Figure 1. Articular cartilage (indicated by the arrow in (a)) and two kinds of PVA hydrogels as artificial cartilage. PVA: poly(vinyl alcohol).

its outer radius is 5 mm. A commercial package ABAQUS (6.8-4) was used in this study. The biphasic tissue was modelled by CPE4RP (four-node bilinear displacement and pore pressure, reduced integration with hour glass control) elements, and a mesh was chosen as 0.1-mm thick with 0.1 mm on surface. The bottom of the model was fixed and impermeable. The other surfaces were not fixed and basically permeable except for the contact region. The load of 0.5 N/mm (for articular cartilage) or 0.2 N/mm (for PVA) was applied at the centre of the cylindrical cartilage or PVA hydrogel surface with a ramp time of 1 s, and then the load was held constant for further 508 s (for cartilage) or 292 s (for PVA) during reciprocation motion. For stroke of 8 mm at period of 4 s, the sliding speed is 4 mm/s, where the hydrodynamic action diminishes. The changes in interstitial fluid pressure and stress in solid phase during reciprocating motion were examined by similar method to that in the previous paper for reciprocating rigid cylindrical indenter on flat cartilage plate.[17] The friction coefficient for solid-to-solid contact μ_{solid} between the geometrical rigid plate and the solid phase was set to 0.01 or 0.2.

Articular cartilage model. The biphasic FE analysis for articular cartilage was conducted by using inhomogeneous depth-dependent apparent Young's modulus of solid phase,[18] strain-dependent permeability (compaction effect)[19,40] and collagen reinforcement in tensile strain.[19] Material properties were specified by curve fitting comparing FE calculation with experimental time-dependent reaction force of the cylindrical indenter. The variables derived from the curve fitting on FE calculation were described in the previous paper.[14]

The horizontal and vertical fibrils were represented by spring element SPRINGA (axial spring between two nodes, whose line of action is the line joining the two nodes) of the software, in which the spring elements were configured to generate reaction force only in the tensile direction. The stiffness K of the spring elements was simplified to the uniform value over the tissue and both in horizontal and vertical direction.

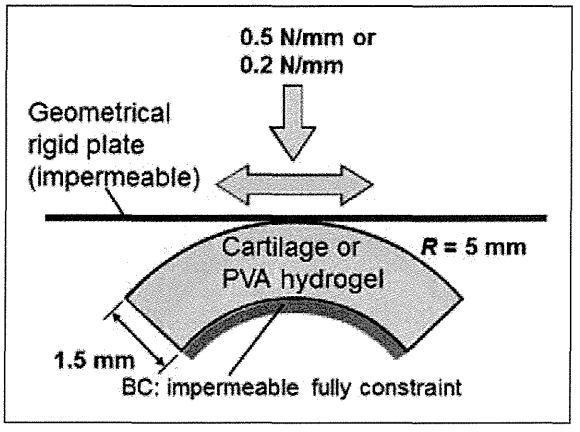

Figure 2. Two-dimensional model for biphasic FE analyses. FE: finite element.

Artificial hydrogel cartilage model. The material properties of PVA hydrogels were estimated from the stress-relaxation tests of cuboid (10 mm × 6 mm × 4 mm) under uni-axial compression at definite deformation after average stress of 0.1 MPa had been attained as indicated by Yamaguchi et al.[41] The compressive stress during stress relaxation $f(t)$ is shown as given below.

$$f(t) = \frac{3G\varepsilon_{z0}}{1 + G/3K(1 - \exp(-t/t_{rel}))} \quad (1)$$

where G is the shear modulus of rigidity, K the bulk modulus of elasticity, ε_{z0} the compressive strain and t_{rel} the relaxation time. G, K and t_{rel} are estimated by fitting with this formula to stress-relaxation curve. The permeability k is estimated from the following formula

$$k = C\frac{W^2}{K\, t_{rel}} \quad (2)$$

where W is the shorter width of specimen and C the constant.

$$C = 3/16 \quad \text{for } K \ll G \quad (3)$$

$$C = 1/\pi^2 \quad \text{for } K \gg G \quad (4)$$

Results

Experimental results on frictional behaviours for articular cartilage on reciprocating glass plate

As mentioned in the previous papers[14–16] on biphasic lubrication for articular cartilage in reciprocating tests, low friction is sustained for reciprocation with migrating contact area on cartilage surface such as the reciprocation of rigid indenter on articular cartilage plate. On the other hand, the friction was low at start but gradually increased to higher level for articular cartilage under continuous loading on the reciprocating rigid plate. This time-dependent frictional behaviour is observed for friction of intact articular cartilage on the reciprocating glass plate in saline as shown in Figure 3. However, the level of final friction at 36-m sliding changes depending on the lubricant constituents.[16] If a simulated synovial fluid such as 0.5 wt% HA solution containing 0.01 wt% DPPC, 1.4 wt% albumin and 0.7 wt% γ-globulin was supplied as lubricant, very low friction was maintained until 36-m sliding (Figure 3), for which minimum wear of cartilage was observed. This lubricant contains main important constituents in natural

synovial fluid. Thus, this result exhibits the superior lubricity in articular cartilage combined with synovial fluid as boundary lubricant. In this paper, the relationship between biphasic lubrication and boundary lubrication was examined on the basis of biphasic FE analysis in the following section.

Biphasic FE analysis on frictional behaviours for articular cartilage on reciprocating glass plate

The time-dependent changes in interstitial fluid pressure and von Mises stress of solid phase in simulated reciprocating tests for articular cartilage with $\mu_{solid} = 0.2$ were explained based on biphasic FE analysis in the previous paper.[14] In this paper, therefore, time-dependent behaviour of articular cartilage for $\mu_{solid} = 0.01$ was examined as shown in Figure 4. It is worth noting that at start immediately after loading, the interstitial fluid pressure is significantly high and von Mises stress is low, particularly the stress on the surface is extremely low. With further rubbing, the fluid pressure significantly subsides accompanied with further deformation at 508 s run under continuous loading. However, the stress level for $\mu_{solid} = 0.01$ (corresponding to simulated synovial fluid) is not so much high compared with the stress for $\mu_{solid} = 0.2$ (corresponding to saline).[14] The black area for fluid pressure at 508 s in Figure 4(a) corresponds to negative pressure, which facilitates the flowing in but may not contribute to the fluid load support.

Time-dependent frictional behaviours are estimated from biphasic FE analysis for two conditions for μ_{solid} as 0.01 and 0.2, as shown in Figure 5, in which the changes in partitioning of fluid load support are shown at start and at 507 s. For $\mu_{solid} = 0.2$, the fluid load support is changed from 90.5% to 27%.

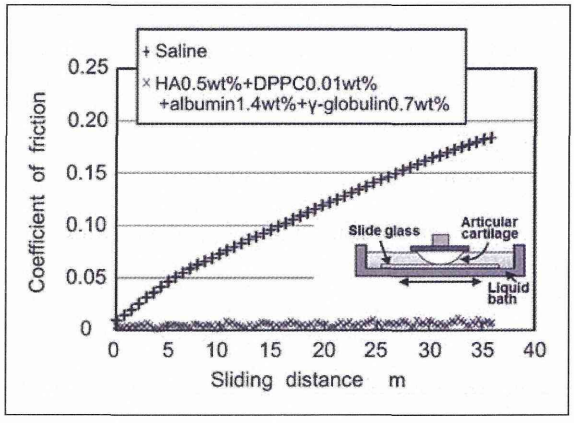

Figure 3. Influence of lubricants on changes in friction of intact articular cartilage against glass plate in reciprocating tests at 9.8 N.

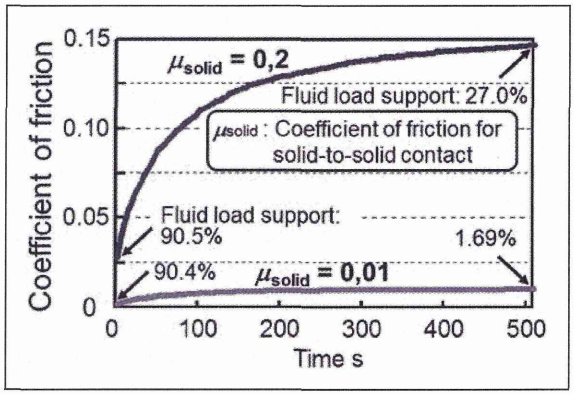

Figure 5. Influence of coefficient of friction for solid-to-solid contact on changes in friction of articular cartilage against glass plate (biphasic FE analysis). FE: finite element.

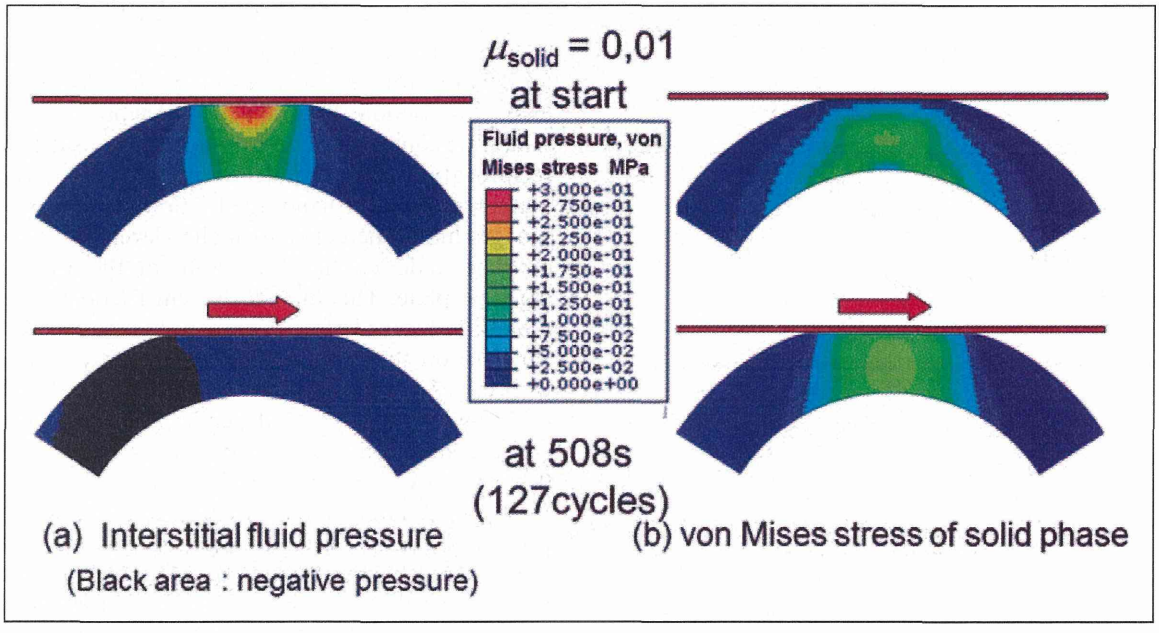

Figure 4. Changes in interstitial fluid pressure and von Mises stress in articular cartilage in reciprocating motion at low-friction condition (biphasic FE analysis). FE: finite element.

For $\mu_{solid} = 0.01$, it is changed from 90.5% to 1.69%, but the coefficient of friction is sustained as about 0.01. This low friction for $\mu_{solid} = 0.01$ indicates the importance of surface lubricity for low friction with boundary lubrication under continuous load, which corresponds to result for a simulated synovial fluid in Figure 3.

Experimental results on frictional behaviours for artificial cartilage on reciprocating glass plate

In reciprocating tests until 140-m sliding for articular cartilage and PVA hydrogel specimens against flat glass plate at continuous loading of 2.94 N, these specimens different in structures and properties revealed similar or different frictional behaviours in lubrication with saline as shown in Figure 6. The articular cartilage and freeze-thawing PVA hydrogel exhibited low-initial friction and gradual increase, where freeze-thawing PVA showed higher friction than that for cartilage. In contrast, cast-drying PVA exhibited very low friction with a slower increase. These differences are considered to be related to the difference in biphasic lubrication as mentioned later.

Next, to improve frictional behaviours in freeze-thawing PVA, the effect of lubricant constituents was examined. As shown in Figure 7, first, the influence of addition of single constituents in lubricant was evaluated in repeated reciprocating tests including 5 min unloading of 9.8 N after 36-m sliding and restart, where the effect of recovering of hydration, adsorbed film formation and deformation can be compared.[15] It is confirmed that the addition of protein affects friction adversely but the addition of HA and DPPC contributes to remarkable reduction in friction. Figure 8 shows the effect of HA solutions containing DPPC with and without proteins on friction. The combination of HA and DPPC with and without proteins can maintain low-friction level as clearly shown in Figure 9. Subsequently, the wear-resistance properties were examined. It is noticed that 0.5 wt% HA solution containing 0.01 wt% DPPC, 1.4 wt% albumin and 0.7 wt% γ-globulin showed minimum wear (Figure 9) similarly to articular cartilage. Thus, the reduction in both friction and wear for freeze-thawing PVA hydrogel is possible with the aid of synovia in human joint environment. However, changes in synovia constituent can happen in the diseased human body, and in such case, other lubrication mechanism becomes important as a robust system. Therefore, the role of biphasic lubrication is discussed in the next section.

Biphasic analysis on frictional behaviours for artificial cartilage on reciprocating glass plate

The mechanical properties of two PVA hydrogel specimens were estimated by the stress-relaxation test mentioned above as shown in Table 1.[41] It is noteworthy that the cast-drying hydrogel has lower permeability as two-order than freeze-thawing hydrogel.

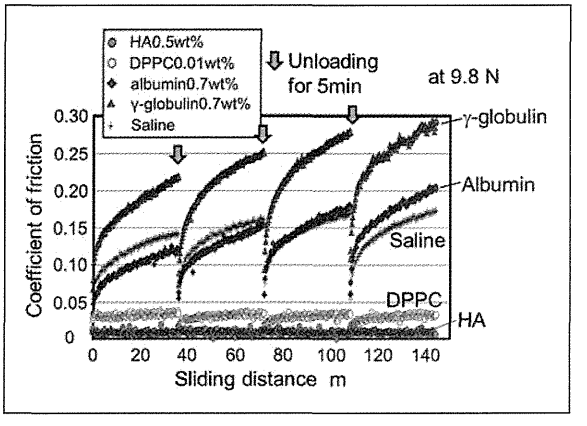

Figure 7. Influence of each synovia constituent on changes in friction of freeze-thawing PVA hydrogel against glass plate. PVA: poly(vinyl alcohol).

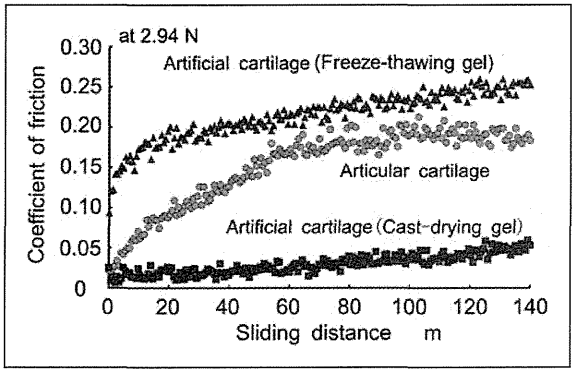

Figure 6. Changes in friction of intact articular and artificial cartilage specimens against glass plate in saline.

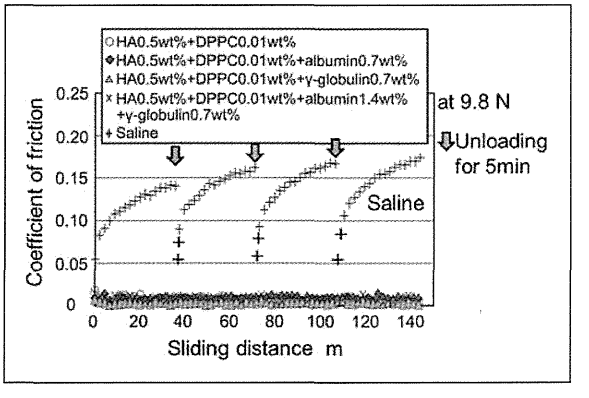

Figure 8. Influence of combination of synovia constituents on changes in friction of freeze-thawing PVA hydrogel against glass plate. PVA: poly(vinyl alcohol).

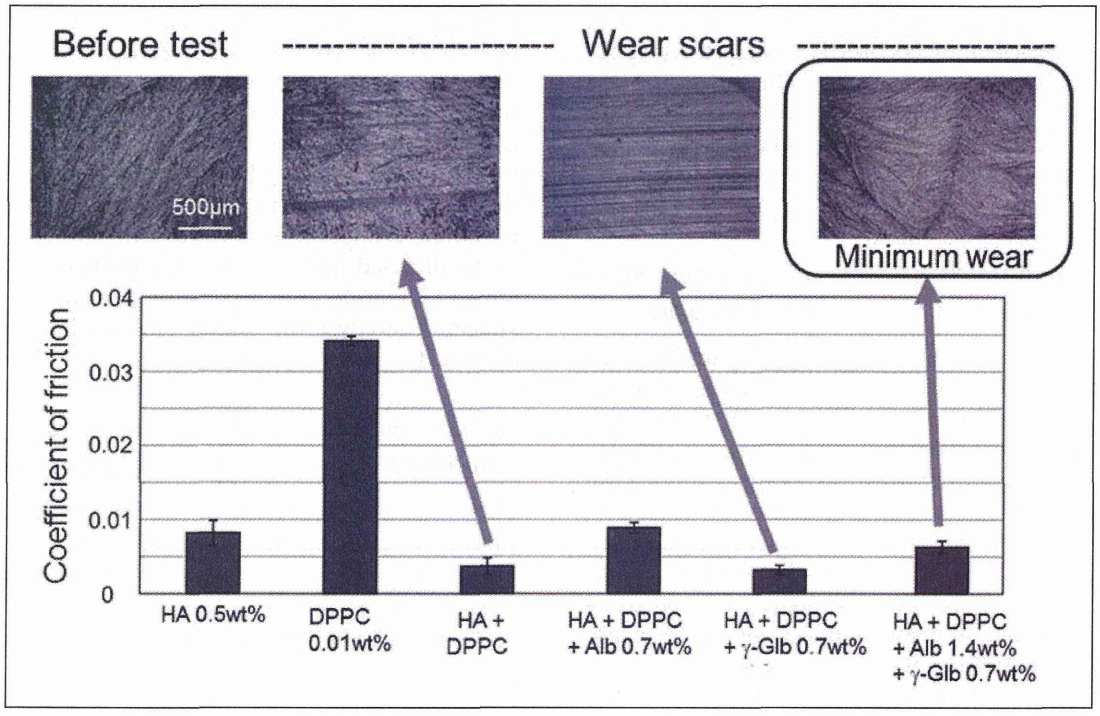

Figure 9. Influence of lubricants on average coefficient of friction after each 36 m sliding and worn surfaces of freeze-thawing PVA hydrogel in reciprocating tests at 9.8 N. PVA: poly(vinyl alcohol).

Table 1. Properties of PVA hydrogels.

Preparation method for PVA hydrogel	Permeability (m^4/Ns)	Young's modulus (kPa)	Poisson's ratio
Freeze-thawing	2.0×10^{-13}	110	0
Cast-drying	2.4×10^{-15}	190	0.41

PVA: poly(vinyl alcohol).

The permeability of cast-drying hydrogel has similar level to that of natural articular cartilage.

The interstitial fluid pressure after 292 s for two kinds of solid-to-solid friction conditions as 0.01 and 0.2 in reciprocating test is shown in Figure 10. The cast-drying PVA hydrogel maintains significant pressure even after 292 s, but in freeze-thawing PVA, the fluid pressure was remarkably reduced. For both PVA hydrogels, high friction of solid-to-solid sustained the fluid pressure levels to higher with larger deformation than those for low μ_{solid}. Therefore, caution is demanded because contrary to expectation, the lower surface friction accelerates an increase in solid-to-solid contact. The changes in load supports by fluid and solid phases are exhibited in Figure 11.

The estimated frictional behaviours for PVA hydrogels in reciprocating tests are shown in Figure 12. It is noticed that low-friction property of surfaces (solid-to-solid) maintains the sliding friction under significantly low level. Even for high μ_{solid}, cast-drying PVA can bring the gradual decreasing in friction, probably due to rising of fluid load support from 74% to 80% in biphasic analysis (Figure 11).

Discussion

In this paper, as one example of superior lubricity of articular cartilage, it was described that the addition of lubricant containing important lubricating constituents in synovial fluid can reduce friction (Figure 3) and minimize wear[16] for cartilage even under severe rubbing condition at continuous loading. Under this reciprocating condition, the role of fluid load support diminishes with rubbing (Figures 4 and 5), which means the loss of biphasic lubrication mechanism as indicated above. In natural synovial joints, it is expected that the other lubrication mechanism will alternate as an active one after weakening of biphasic lubrication effect, as suggested by the adaptive multimode lubrication mechanism.[3,13,14] The boundary lubrication based on appropriate adsorbed film formation on cartilage surface appears to become

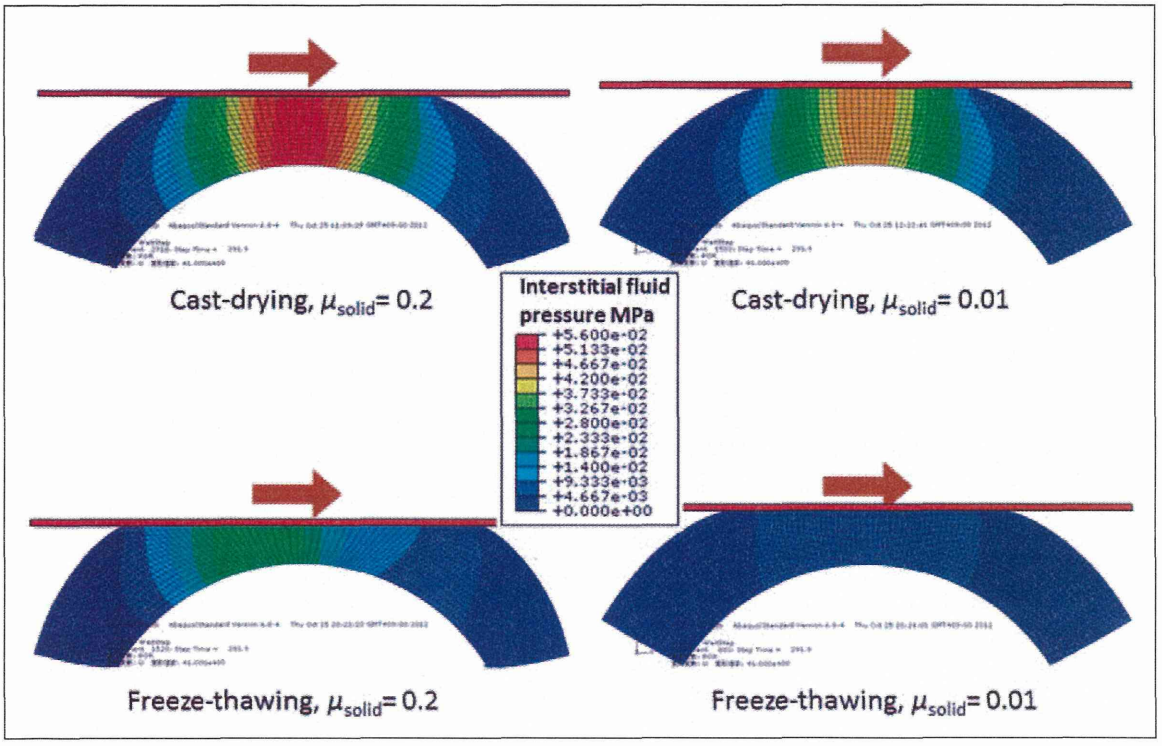

Figure 10. Interstitial fluid pressure in PVA hydrogels at 292 s in reciprocating tests (biphasic FE analysis). FE: finite element; PVA: poly(vinyl alcohol).

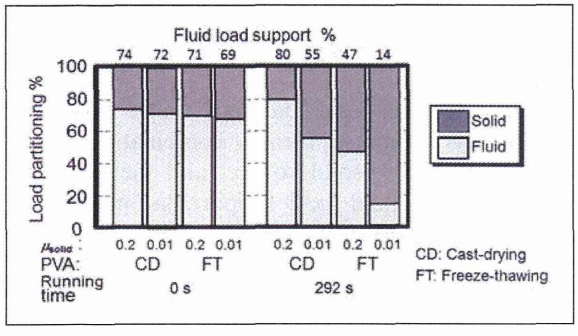

Figure 11. Changes in load support in PVA hydrogels (biphasic FE analysis). FE: finite element; PVA: poly(vinyl alcohol).

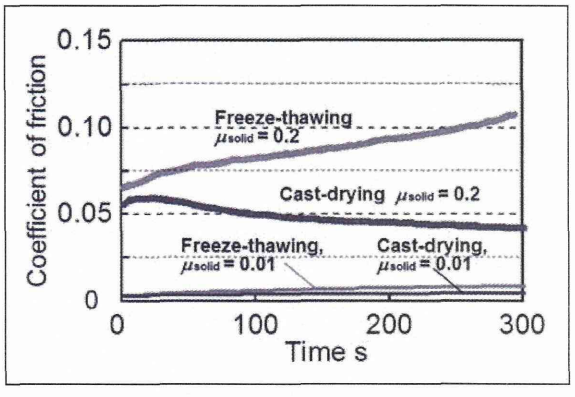

Figure 12. Changes in friction of PVA hydrogels (biphasic FE analyses). FE: finite element; PVA: poly(vinyl alcohol).

effective by supplying of important lubricating constituents of appropriate concentration and ratio (0.5 wt% HA, 0.01 wt% DPPC, 1.4 wt% albumin and 0.7 wt% γ-globulin) into lubricant, which corresponds to low value of μ_{solid}. In this paper, the possibility in which similar mechanism is expected to be applicable for artificial hydrogel cartilage is discussed as below.

As artificial hydrogel cartilage containing high-water content, two kinds of hydrogel showed quite different time-dependent frictional behaviours in reciprocating tests in saline (Figure 6). In the measurement of time-dependent changes of contact area in static loading test,[42] freeze-thawing PVA hydrogel showed initial abrupt deformation and subsequent steady state. Cast-drying PVA showed similarly initial abrupt deformation and maintained steady state but its compressive deformation was lower than freeze-thawing PVA. In contrast, natural articular cartilage showed gradual increase in deformation, as suggested by usual biphasic model. These phenomena are likely to depend on the permeability and elastic modulus of hydrogel. Detailed analysis for difference in deformation behaviours between PVA hydrogels and articular cartilage should be examined in further study.

The high friction and constant compressive deformation of freeze-thawing PVA hydrogel is considered to be due to biphasic properties with high permeability (Table 1). The interstitial fluid pressure in

freeze-thawing PVA remarkably diminished after 292 s running as shown in Figure 10, and therefore the fluid load support became small (Figure 11). The friction in saline is expected to increase gradually as indicated by the curve for $\mu_{solid} = 0.2$ (Figure 12). Even in case of low fluid load support, it was demonstrated in experiment that another lubrication mechanism as boundary lubrication with important synovia constituents enables to reduce friction remarkably (Figures 7 to 9) and minimize wear (Figure 9). The comparison of experimental results (Figures 6 to 8) with biphasic FE analysis (Figure 12) clearly demonstrates the acceptable correspondence of both cases for high or low friction by considering appropriate selection of 0.2 or 0.01 as μ_{solid}. Therefore, it is indicated that the usage of freeze-thawing PVA lubricated with a simulated synovial fluid is a possible solution for clinical application.

Next, the friction behaviours of the cast-drying PVA hydrogel should be considered. As shown in Figure 6, the low friction of cast-drying PVA hydrogel during sliding duration in saline for a long time is very attractive. This property appears to be derived from low permeability (Table 1) of biphasic material. As shown in Figure 10, the interstitial fluid pressure sustained even after 292 s running for cast-drying PVA. Its fluid load support increased after 292 s running for $\mu_{solid} = 0.2$ (Figure 11). Therefore, friction can be reduced after 292 s running for $\mu_{solid} = 0.2$ in biphasic analysis (Figure 12). However, the frictional behaviour in experiment (Figure 6) is different from the estimated curves for $\mu_{solid} = 0.2$ or 0.01. The appropriate selection for $\mu_{solid} = 0.05$ or so may bring favourable correspondence.

Thus, it is worthy of remark that the permeability regulated by the material properties and structures of hydrogel will mainly control the biphasic fluid flow behaviour. The material properties and structures in both PVA hydrogels appear to depend on the structure controlled by hydrogen bond. The model for microstructure in PVA hydrogel was proposed by Otsuka and Suzuki[38] as shown in Figure 13.

The formation of hydrogen bonds and microcrystallites was identified using X-ray diffraction (XRD) technique, Fourier transform infrared (FTIR) spectroscopy and measurements of the swelling ratio under repeated water exchanges.[43] In Figure 13, d, D and L are deduced from the diffraction peaks at XRD spectra. Small-angle scattering indicates that the distance between microcrystallites L in freeze-thawing PVA hydrogel is shorter than in cast-drying PVA hydrogel. As shown in Figure 1, the transparency of cast-drying hydrogel indicates its uniform network structure, and the milky white appearance of freezing-thawing hydrogel suggests the heterogeneous network structure. In Figure 14, the schematic models based on personal communication from E Otsuka and A Suzuki[42] for these hydrogels are shown accompanied with atomic force microscopy (AFM) surface images of their swollen states in water. The network

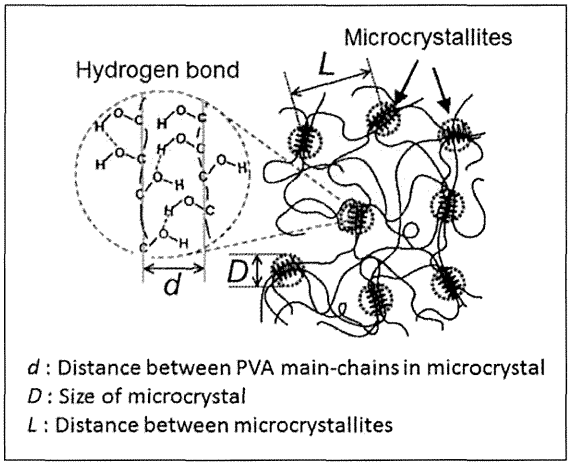

Figure 13. Network structure of PVA hydrogels crosslinked by microcrystallites.[38]
PVA: poly(vinyl alcohol).
Source: reproduced with permission of John Wiley & Sons, Inc.

is generally composed of microcrystallites and amorphous zones. It is suggested that the fluid flows out rapidly from freeze-thawing PVA hydrogel, which is composed of microcrystallites and considerable amorphous zones, as indicated by high permeability (Table 1), and porous texture in AFM image (Figure 14). On the contrary, in cast-drying PVA hydrogel with low permeability, the fluid retained inside of gel with slow flows out, and thus the interstitial fluid pressure maintains for longer time under reciprocating tests.

Friction for biphasic materials under lubricated conditions is estimated from a combination of the friction for solid-to-solid contact and the negligibly low friction for fluid load support, as indicated in formula for friction by Ateshian et al.,[44,45] where high partitioning of load support by fluid phase contributes to lowering in friction. Changes in load support in compliant hydrogels estimated on the basis of biphasic FE analysis for reciprocating test under continuous loading are shown in Figure 11, which depend on not only permeability but also friction level for solid-to-solid contact. In saline where the friction for solid-to-solid contact is high, the higher load support by interstitial fluid pressure maintained with low permeability for cast-drying gel gives lower friction, while the limited load support by low-fluid pressure attributable to faster fluid exudation caused by higher permeability for repeated freeze-thawing gel gives high friction, as shown in Figure 12. The lower friction for cast-drying gel in saline (Figure 6) appears to be brought about by superior surface lubricity as $\mu_{solid} = 0.05$ or so as mentioned above. The smooth surface of cast-drying PVA may contribute to the reduction of friction in saline by suppressing interaction between rubbing surfaces. The rough and porous surface of freeze-thawing PVA may enhance interaction between rubbing surfaces in saline and

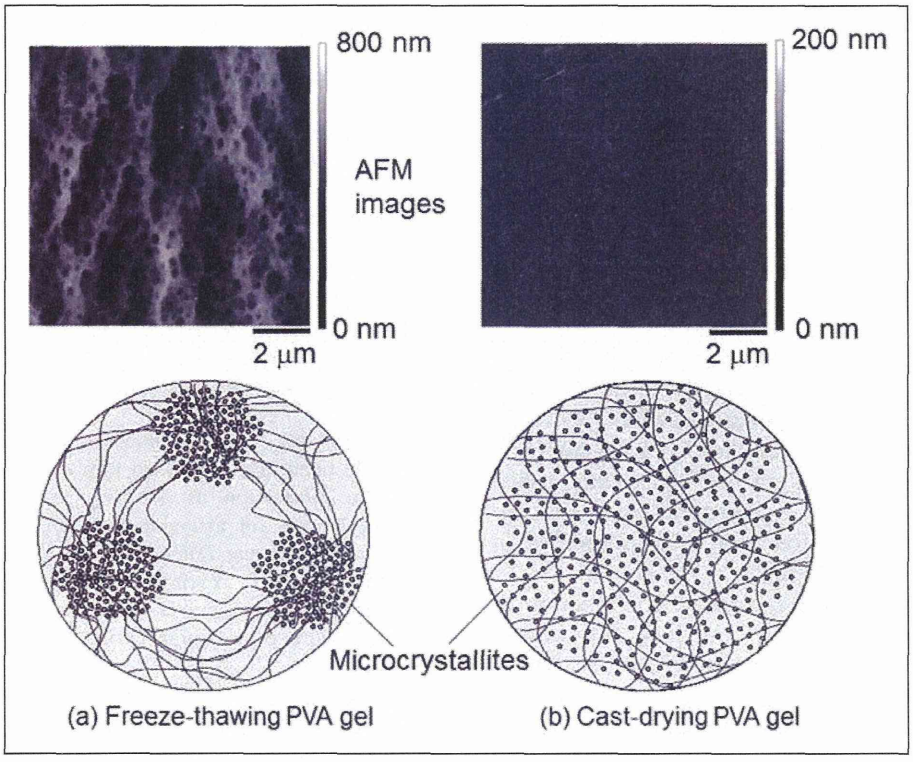

Figure 14. AFM images in water and schematic models[42] for two kinds of hydrogel structures. AFM: atomic force microscopy.

increase friction, but improve the adsorbed film formation under lubricated condition with a simulated synovial fluid and reduce friction (Figures 8, 9 and 12). Elucidation of the exact lubrication mechanism for hydrogel should be continued in further studies.

Other improving methods for properties of PVA hydrogel are to additionally control the nanoscopic structure, to reinforce the structure with fibrous element or other method and thus to enhance biphasic properties for efficient lubrication and load-carrying property. The freeze-thawing and cast-drying PVA hydrogels based on hydrogen-bonding network as physical bonding prepared without any additives or irradiative stimulus have superiority in safety in human body. The possibility of restoration with hydrogen bonding in case of local fracture is a favourable property.

The main purpose of this study was to examine friction differences between two kinds of hydrogels, but wear differences become more important in clinical application. In authors' related research on reciprocating tests with an alumina ball against flat PVA hydrogel plates in pure water (Suzuki et al.[46]), cast-drying gel with low permeability showed lower wear and lower friction than freeze-thawing gel with high permeability. The superiority of cast-drying gel appears to be caused by its better biphasic property in water. However, in this study, freeze-thawing gel exhibited minimum wear in simulated synovia lubricant as HA solution containing appropriate concentration of albumin, γ-globulin and DPPC in reciprocating tests under continuous loading. This indicates the effectiveness of surface protection by adsorbed film formed on freeze-thawing gel surface. The wear behaviour of cast-drying gel in various lubricants should be examined in future studies.

For the clinical application of PVA hydrogel, durability, synergistic interaction with lubricants, ease of production, formability, appropriate fixation methods and other properties are required. In particular, the establishment of appropriate design in consideration of a multimode lubrication mechanism is required not only for low friction but also for zero-wear and high-fatigue resistance in the human body. To evaluate predictively the in vivo behaviours of two kinds of hydrogels, the various tests such as reciprocating tests and simulator tests should be conducted under biomechanically simulated environmental conditions. The desirable in vivo performance of PVA hydrogel implanted in rabbit knee joint in ongoing tests with biomedical research group suggests the feasibility of clinical application. In the next step, the authors plan to apply a hybrid hydrogel (Suzuki et al.[46]) composed of cast-drying PVA on freeze-thawing PVA as another candidate material for the artificial cartilage with superior lubricity.

Conclusion

To explore the superior lubricity of articular cartilage and artificial hydrogel cartilage, time-dependent frictional behaviours in natural articular cartilage and

two kinds of PVA hydrogels prepared by repeated freeze-thawing method and cast-drying method were examined in reciprocating tests and biphasic FE analyses.

Articular cartilage showed initial low friction and gradual increase in saline lubrication where biphasic fluid load support mechanism subsides with rubbing as indicated by biphasic FE analysis. However, the addition of a simulated synovial fluid enabled the superior lubrication by appropriate adsorbed film formation in boundary lubrication mode.

In artificial cartilage materials in saline, cast-drying PVA with low permeability clearly showed significantly lower friction than freeze-thawing PVA with high permeability. For freeze-thawing PVA hydrogel in which biphasic lubrication mechanism diminished with rubbing, the supply of appropriate synovia constituents improved friction and wear properties in boundary lubrication mode.

It was shown that the synergistic combination of biphasic lubrication and boundary lubrication becomes effective to sustain superior lubricity in articular cartilage and PVA hydrogels even at slow movement under continuous loading.

Funding

The authors thank the financial support given by the Grant-in-Aid for Specially Promoted Research of Japan Society for the Promotion of Science (Kaken: 23000011).

References

1. Dowson D. Modes of lubrication in human joints. *Proc IMechE* 1966–1967; 181(Pt 3J): 45–54.
2. Unsworth A, Dowson D and Wright V. Some new evidence on human joint lubrication. *Ann Rheum Dis* 1975; 34(4): 277–285.
3. Murakami T. The lubrication in natural synovial joints and joint prostheses. *JSME Int J Ser III* 1990; 33(4): 465–474.
4. Dowson D and Jin ZM. Micro-elastohydrodynamic lubrication of synovial joints. *Eng Med* 1986; 15: 65–67.
5. Forster H and Fisher J. The influence of loading time and lubricant on the friction of articular cartilage. *Proc IMechE Part H: J Engineering in Medicine* 1996; 210: 109–119.
6. Ateshian GA. Theoretical formulation for boundary friction in articular cartilage. *J Biomech Eng* 1997; 119(1): 81–86.
7. Klein J. Molecular mechanisms of synovial joint lubrication. *Proc IMechE Part J: J Engineering Tribology* 2006; 220: 691–710.
8. Ikeuchi K. Origin and future of hydration lubrication. *Proc IMechE Part J: J Engineering in Medicine* 2007; 221: 301–305.
9. Swann DA, Hendren RB, Radin EL, et al. The lubricating activity of synovial fluid glycoproteins. *Arthrit Rheum* 1981; 24: 22–30.
10. Hills BA. Oligolamellar lubrication of joints by surface active phospholipids. *J Rheum* 1989; 16(1): 82–91.
11. Higaki H and Murakami T. Role of constituents in synovial fluid and surface layer of articular cartilage in joint lubrication (part 2) the boundary lubricating ability of proteins. *Jpn J Tribol* 1996; 40(7): 691–699.
12. Murakami T, Sawae Y, Horimoto M, et al. Role of surface layers of natural and artificial cartilage in thin film lubrication. In: D Dowson, M Priest, CM Taylor, et al. (eds) *Lubrication at the frontier*. Amsterdam: Elsevier, 1999, pp.737–747.
13. Murakami T, Higaki H, Sawae Y, et al. Adaptive multimode lubrication in natural synovial joints and artificial joints. *Proc IMechE, Part H: J Engineering in Medicine* 1998; 212: 23–35.
14. Murakami T. Importance of adaptive multimode lubrication mechanism in natural and artificial joints. *Proc IMechE Part J: J Engineering Tribology* 2012; 226: 827–837.
15. Murakami T, Nakashima K, Yarimitsu S, et al. Effectiveness of adsorbed film and gel layer in hydration lubrication as adaptive multimode lubrication mechanism for articular cartilage. *Proc IMechE Part J: J Engineering Tribology* 2011; 225: 1174–1185.
16. Murakami T, Yarimitsu S, Nakashima K, et al. Influence of synovia constituents on tribological behaviors of articular cartilage. *Friction* 2013; 1(2): 150–162.
17. Sakai N, Hagihara Y, Furusawa T, et al. Analysis of biphasic lubrication of articular cartilage loaded by cylindrical indenter. *Tribol Int* 2012; 46: 225–236.
18. Hosoda N, Sakai N, Sawae Y, et al. Depth-dependence and time-dependence in mechanical behavior of articular cartilage in unconfined compression test under constant total deformation. *J Biomech Sci Eng* 2008; 3: 209–220.
19. Li LP, Soulhat J, Buschmann MD, et al. Nonlinear analysis of cartilage in unconfined ramp compression using a fibril reinforced poroelastic model. *Clin Biomech* 1999; 14: 673–682.
20. Willert HJ and Semlitsch M. Reaction of the articular capsule to wear products of artificial joint prostheses. *J Biomed Mater Res* 1977; 11: 157–164.
21. Ingham E and Fisher J. The role of macrophages in osteolysis of total joint replacement. *Biomaterials* 2005; 26: 1271–1286.
22. Williams PA, Yamamoto K, Masaoka T, et al. Highly crosslinked polyethylenes in hip replacements: improved wear performance or paradox? *Tribol Trans* 2007; 50: 277–290.
23. Tomita N, Kitakura T, Onmori N, et al. Prevention of fatigue cracks in ultrahigh molecular weight polyethylene joint components by the addition of vitamin E. *J Biomed Mater Res (Appl Biomater)* 1999; 48: 474–478.
24. Moro T, Takatori Y, Ishihara K, et al. Surface grafting of artificial joints with a biocompatible polymer for preventing periprosthetic osteolysis. *Nat Mater* 2004; 3: 829–836.
25. Dowson D. Are our joint replacement materials adequate? In: *Proceedings of the IMechE International Conference*, 1989, C384/KN1: 1–5.
26. Unsworth A, Pearcy MJ, White EFT, et al. Soft layer lubrication of artificial hip joints. *Proc IMechE* 1987; C219/87: 715–724.
27. Murakami T, Ohtsuki N and Higaki H. The adaptive multimode lubrication in knee prostheses with compliant layer during walking motion. In: D Dowson, et al.